Perspectives for Photoelectron Spectroscopy of Solids using Hard X-rays for Excitation

László Kövér

Institute of Nuclear Research of the Hungarian Academy of Sciences

18/c Bem tér, H-4026 Debrecen, Hungary

OUTLINE

I. Introduction
- Motivations & significance
- HAXPES, excitations accompanying photoionization in solids

II. Photoelectrons induced by hard X-rays
- Photoemission : energy dependence of the non-dipole effects
- Photoemission : effects of atomic recoil

III. Physical parameters characterizing the electron transport processes within the solid
- Electron transport parameters obtainable from spectra of energetic electrons backscattered from solids
- Effective Attenuation Lengths (0.5- 15 keV): comparison of predictions and experiments
- Intrinsic excitations, role of interferences

IV. Examples of applications
- Analysis of surface/interface nanostructures
- Concentration depth profiles in thin films

V. Summary and perspectives

Introduction

In studies of properties of bulk, surface and interface structures of solids, a strongly increasing use of high energy (2-15 keV) and high energy resolution spectroscopy of electrons induced by synchrotron radiation (Hard X-ray Photoelectron Spectroscopy, HAXPES) can be observed, due to the following advantages:

- Decreased surface and increased bulk sensitivity
- Extended information depth, making accessible the deeply buried interfaces and nanostructures for the sake of studying their physical, chemical and electronic structure
- Possibility for nondestructive concentration depth profiling in a wide (several times 10 nm) thickness range

The high intensity of the synchrotron beams can compensate for the effects of the small photoionization cross sections. In addition, using grazing incidence photon beams, HAXPES can ensure an extreme surface sensitivity.

The accurate information on the electronic structure expected and the quantitative analytical applications, however, request a deeper knowledge on the ionization and excitation processes induced by high energy X-ray photons as well as on the transport of the photoinduced electrons within the solid. Information on the latter can be obtained from REELS spectra.

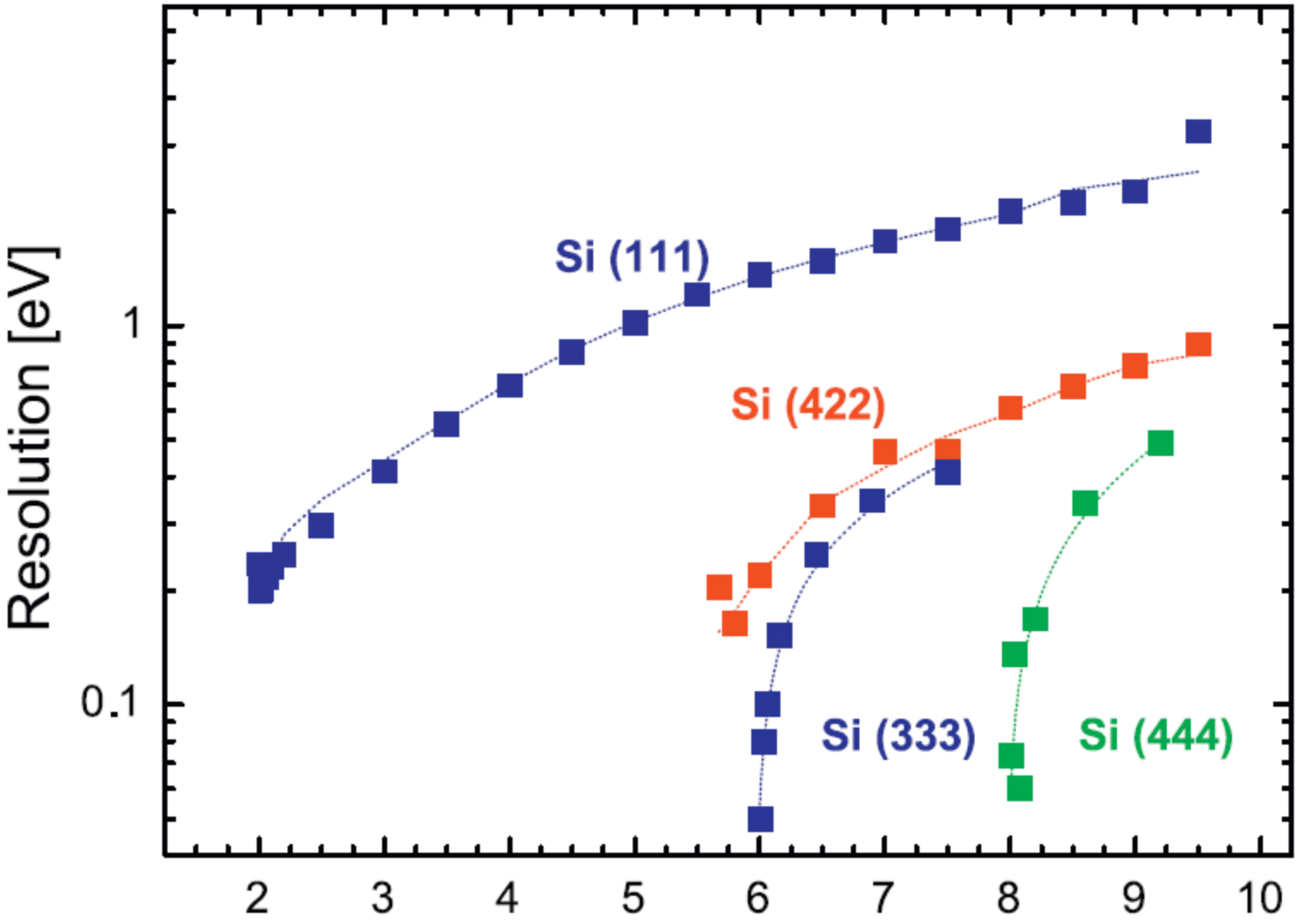

M. Gorgoi et al., Nucl. Instrum. Meth. Phys. Res. A601(2009)48.

HAXPES

Information depth (95 % of the intensity is originated from here) : in the case of 5-15 keV electron energy 50-60 nm can be achieved.

Sensitivity : the subshell photoionization cross sections (PCS) are 2 orders of magnitude smaller, e. g. in the case of 8 keV (Cu Kα), than 1.5 keV (Al Kα) energy photons, however, this decrease, as well as the decrease of the transmission of the spectrometers can be easily compensated for by the photon flux of the a 3rd generation synchrotrons. In the case of increasing photon energy the decrease of the PCS is stronger for high angular momentum electrons, therefore in of valence HAXPES spectra the contribution from e. g. the *d* , or *f* electrons can be decreased in a great extent. E. g. in the case of Fe the 3*d*/4*s* PCS ratio decreases from 60 to 0.1, increasing the photon energy from 0.2 keV to 6 keV.

Surface sensitivity: Only a few % of the intensity originate from the surface (~ Å thick) layer, possibility for the study of the bulk chemical and electronic structure (UHV environment is not a rigorous requirement).

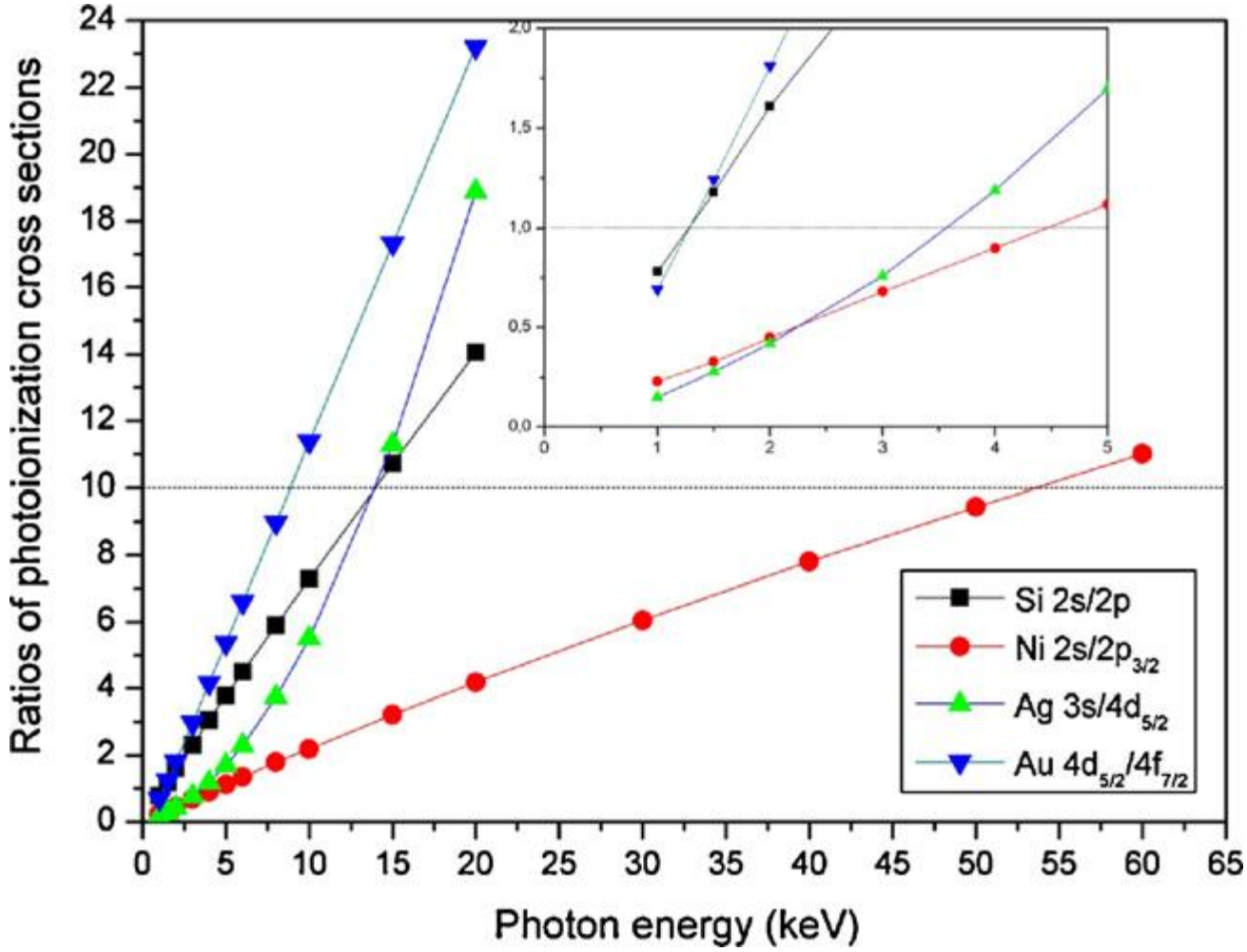

Data: J.H. Scofield, UCRL – 51326, Lawrence Livermore Laboratory, University of California, Livermore, California, 1973.

Photoemission Theories

- **Multipole power series expansion of photon field** (limited number of terms, the first term describes the electric dipole operator, the second the electric quadrupole, the third the magnetic dipole, in the fourth term again the electric dipole) **commonly used** (e.g. M.B. Trzhaskovskaya, V.I. Nefedov, V.G. Yarzhemsky, *Atomic Data and Nuclear Data Tables* **77**(2001)97.).
- **Irreducible tensor expansion of the photon fields** (includes all electric dipole operators, as well as other multipole terms) T. Fujikawa, R. Suzuki, H. Arai, H. Shinotsuka, L. Kövér, *J. Electron Spectrosc. Relat. Phenom*., **159**(2007)14.; R. Suzuki, H. Arai, H. Shinotsuka, T. Fujikawa, *e-J. Surf. Sci. Nanotech.* **3**(2005)373.

In addition to the electric dipole, electric quadrupole and magnetic dipole transitions play important roles in the case of using high-energy X-rays for excitation.

High-energy photoemission: non-dipole effects

The angular distribution of the photoelectrons

The differential photoionization cross section given by Cooper (J. W. Cooper, *Phys. Rev.* **A47** (1993)1841) for linearly polarised photon beam is:

$$\frac{\sigma}{4\pi}\left[1+\beta P_2(\cos\theta)+\left(\delta+\gamma\cos^2\theta\right)\sin\theta\cos\varphi\right] \qquad P_2 = 1/2\,(3x^2 - 1);$$

θ : the angle between the photoelectron detection direction and the polarisation vector;

φ : the angle between the direction of photon propagation and the projection of the photoelectron wave vector in the plane $\perp$ to the polarisation vector.

For circularly polarized or unpolarized photons: $\beta \rightarrow -\beta/2$; $\Theta \rightarrow \underline{\Theta}$; $\gamma \rightarrow \gamma/2$; $\cos^2\Theta \rightarrow \sin^2\underline{\Theta}$; $\sin\Theta\cos\varphi \rightarrow \cos\underline{\Theta}$; where $\underline{\Theta}$ is the angle between the directions of the photons and photoelectrons.

$$\gamma = 18\frac{\rho_s(2)}{\rho_s(1)}\cos\left(\delta_1^A-\delta_2^A\right) \qquad \zeta = \gamma + 3\delta \qquad \delta_l^A:$$

The phase shift of the X-ray absorbing atom *A* (l = 1,2)

$$\rho_s(l) = \int R_l(kr)\left[j_{l-1}(qr)+ j_{l+1}(qr)\right]\frac{dR_s(r)}{dr}r^2dr$$

Radial integrals (l = 1,2)

k : photoelectron momentum ***q*** : photon momentum

T. Fujikawa, R. Suzuki, H. Arai, H. Shinotsuka, L. Kövér, J. Electron Spectrosc. Rel. Phenom. **159**(2007)14.; R. Suzuki, H. Arai, H. Shinotsuka, T. Fujikawa, *e-J. Surf. Sci. Nanotech.* **3,** (2005) 379.

Photoelectron angular distribution

Ge 2s

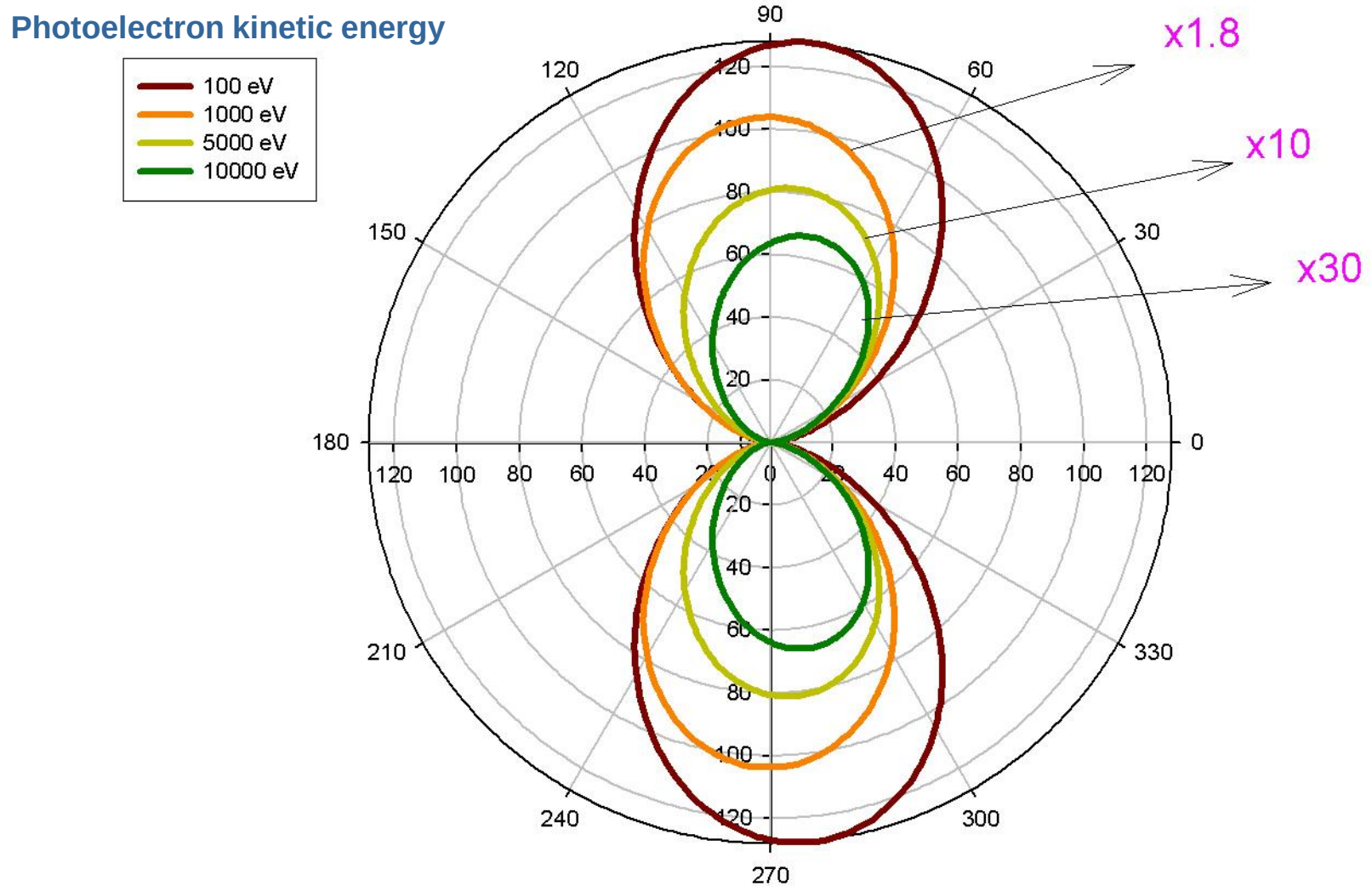

Data: M.B. Trzhaskovskaya, V.I. Nefedov, V.G. Yarzhemsky, *At. Data Nucl. Data Tabl.* **77** (2001) 97; **82** (2002) 257; **92** (2006) 345.

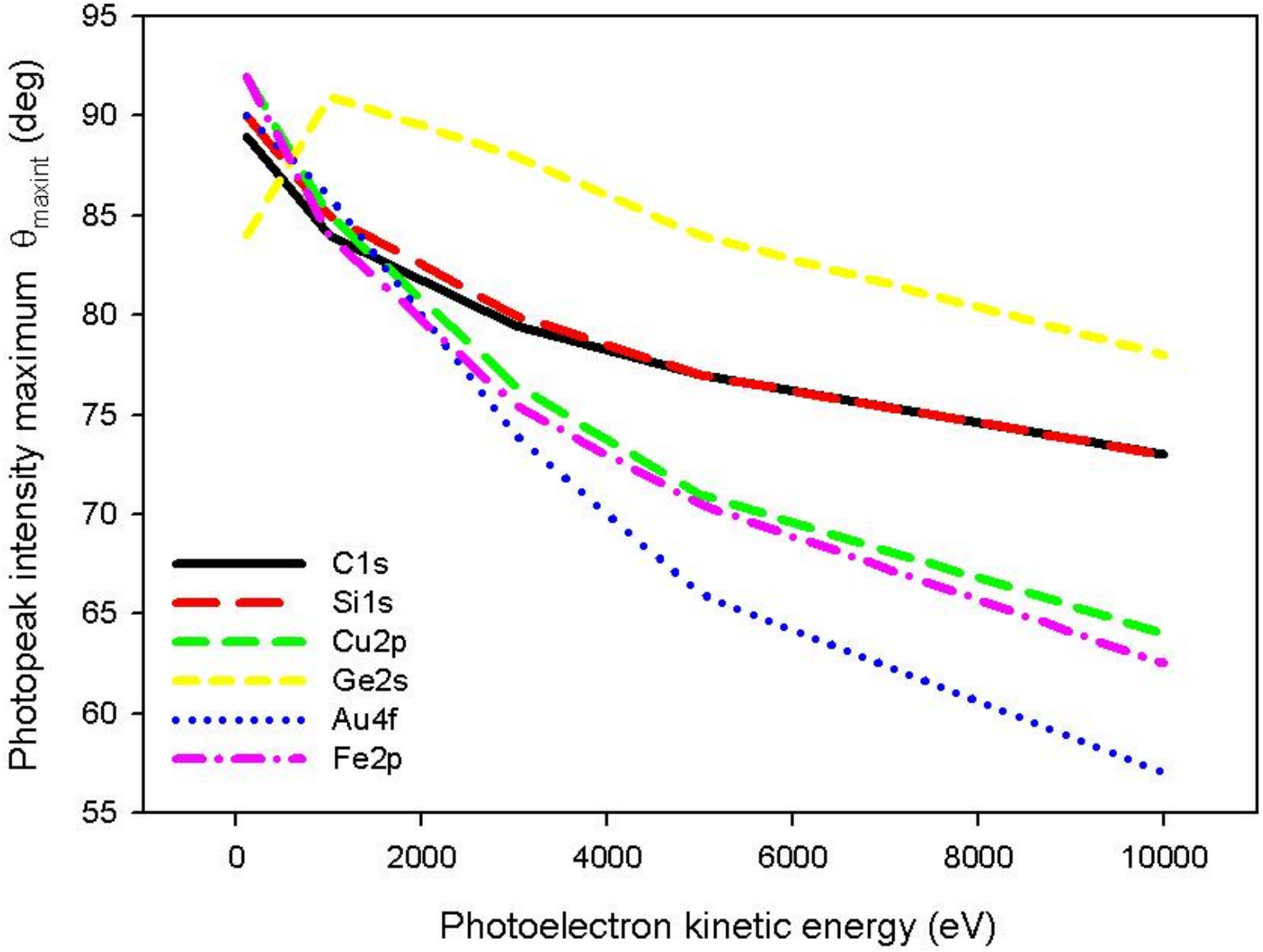

Data: M.B. Trzhaskovskaya, V.I. Nefedov, V.G. Yarzhemsky, *At. Data Nucl. Data Tabl.* **77** (2001) 97; **82** (2002) 257; **92** (2006) 345.

Octupole contribution

Unpolarized photon excitation

$$\frac{d\sigma}{d\Omega} = \frac{\sigma}{4\pi} F$$

$$F = 1 + \beta P_2(\cos\theta) + (\delta + \gamma \cos^2\theta)\sin\theta + \underbrace{\Delta\beta_{unpol} P_2(\cos\theta) + \xi P_4(\cos\theta)}_{f}$$

f : contribution of octupole transitions to photoelectron intensity

$\Delta\beta_{unpol}$ includes interference terms M1-M1, E1-M2, M1-E2, E2-E2, E1-E3, as well as a correction to term E1-E1 of the order of $(kr)^2$

ξ results from E2-E2 and E1-E3 interference

For linearly polarized excitation: $\Delta\beta_{pol}$, η, μ, ξ (identical) $\eta + \mu + \xi = 0$

Unpolarized radiation

Octupole contributions (1s line, Li-Ne): **2-1%** **(E_{kin}=5keV)**

3.4-1.6% **(E_{kin}=10keV)**

Polarized radiation

Octupole contributions (1s line, Li-Ne): **6.0-5.6%** **(E_{kin}=5keV)**

10.6-8.1% **(E_{kin}=10keV)**

M.B. Trzhaskovskaya, V.I. Nefedov, V.G. Yarzhemsky, R. Szargan, *J. Electron Spectrosc. Relat. Phenom.* **133**(2003)65.

Accounting for effects of elastic scattering

For free atoms: $\frac{d\sigma_{nl}}{d\Omega} = \frac{F\sigma_{nl}}{4\pi}$ $F = 1 + \beta P_2(\cos\theta) + (\delta + \gamma\cos^2\theta)\sin\theta$

θ: angle between the photon and photoelectron propagation

For solids: $F_s = a\left[D_1 - \frac{\beta}{4}(3\cos^2\theta - 1) + \left(\frac{\gamma}{2}\sin^2\theta + \delta\right)\cos\theta\right]$

where a = 1-ω ω: single scattering albedo $\omega = \frac{\lambda}{\lambda_{tr} + \lambda}$; λ: IMFP ; λ_{tr} = *tr.*MFP

$\lambda_{tr} = (M\sigma_{tr})^{-1}$; $\sigma_{tr} = \int_{4\pi}(1-\cos\theta)(d\sigma/d\Omega)d\Omega$; M : atomic density; $d\sigma/d\Omega$: diff. cross section for elastic electron scattering

$D_1 = H(\mu,\omega)(1-\omega)^{-0.5}$ $\mu = \cos\alpha$ α: angle of photoelectron emission

$H(\mu,\omega) = \frac{1 + 1.908\mu}{1 + 1.908\mu(1-\omega)^{0.5}}$ (Chandrashekar function)

V.I. Nefedov, V.G. Yarzhemsky, R. Hesse, P. Streubel, R. Szargan, *J. Electron Spectrosc. Relat. Phenom.* **125**(2002)153.

High-energy photoemission: effects of atomic recoil

Model:

- Single site approximation for describing phonon excitations by the recoiled X-ray absorbing atom
- Debye approximation for calculating the energy shift E_r and peak broadening ΔE_r

$$\bar{E}_r = -\frac{Q^2}{2M} \qquad \mathbf{Q} = \mathbf{q} - \mathbf{k} \qquad Q \approx \sqrt{2\left(\hbar\omega - E_B\right)}$$

$$\overline{\left(\Delta E_r\right)^2} = \frac{Q^2\left(k_B T\right)^2}{2M\omega_D}\int_0^{\theta/T} dx x\frac{e^x - 1}{e^x - 1} + \frac{M\omega_D^3 \delta u^2}{\pi}\int_0^{\theta/T} dx \sin^4\left(\frac{\pi T x}{2\theta}\right)\frac{e^x + 1}{x\left(e^x - 1\right)}$$

$FWHM = 2.35\ \sqrt{<(\Delta E_r)^2>}$

$$\frac{\hbar\omega_D}{k_B T} = \frac{\theta}{T}$$

θ: Debye temperature; M: atomic mass;
δu: nuclear displacement after the core-hole production

T. Fujikawa, R. Suzuki, L. Kövér, *J. Electron Spectrosc. Rel. Phenom.* **151,** (2006) 170.
R. Suzuki, H. Arai, H. Shinotsuka, T. Fujikawa, *e-J. Surf. Sci. Nanotech.* **3**(2005) 373.

Recoil shift of photoelectron lines in solids (eV)

	$h\nu$=5 keV	$h\nu$=10 keV
Li 1s	0.56*	0.95
Be 1s	0.34	0.72
C 1s (graphite)	0.25	0.53
Si 1s	0.07	0.16*
Ge 2s	0.03*	0.07*

T. Fujikawa, R. Suzuki, L. Kövér, *J. Electron Spectrosc. Rel. Phenom.* **151**(2006)170; R. Suzuki, H. Arai, H. Shinotsuka, T. Fujikawa, *e-Journal of Surf. Sci. And Nanotechnol.* **3**(2005)373.

*: Estimations based on further approximations

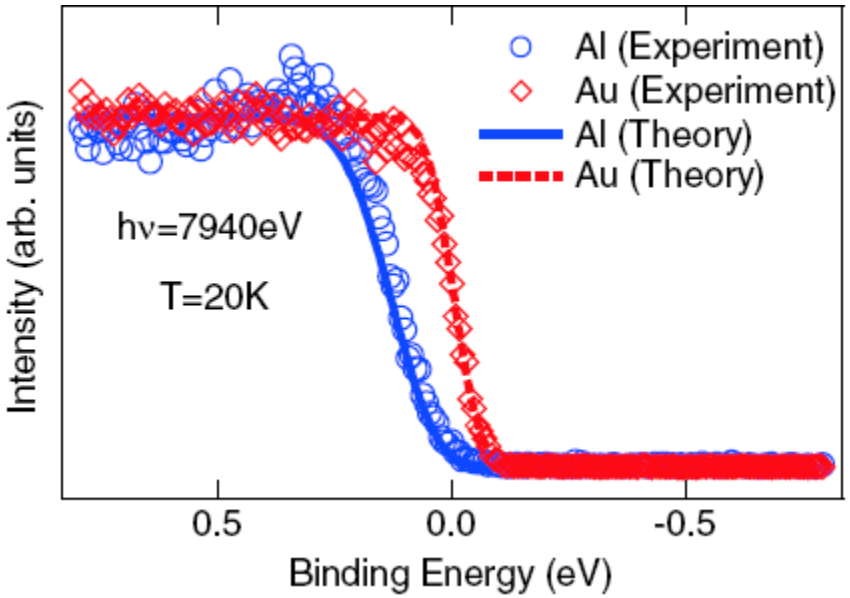

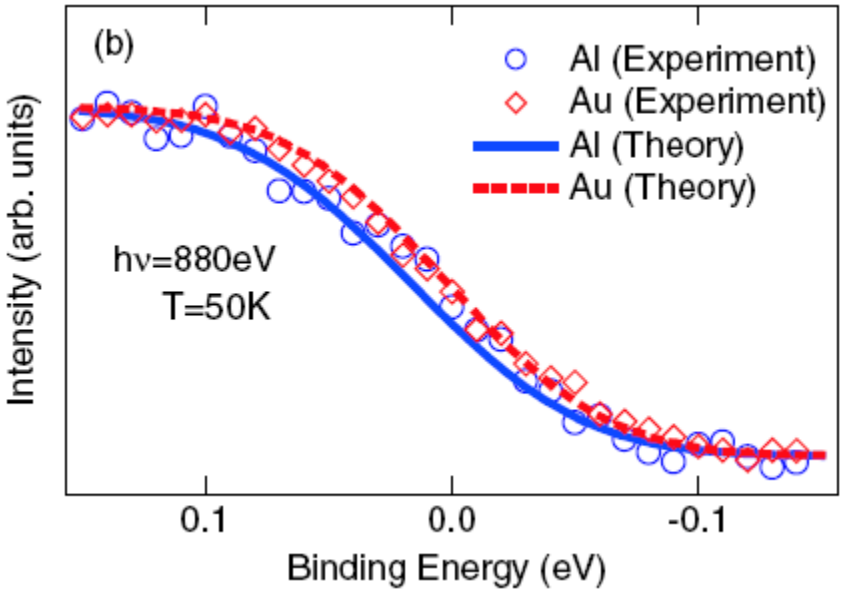

Y. Takata et al., Phys. Rev. Lett. 101(2008)137601.

Types of excitations accompanying photoionization in solids

Extrinsic (during electron transport)
- surface (plasmons)
- bulk (plasmons)

Intrinsic (upon creation of core hole(s))
- shake up, shake off
- collective (plasmons)

Multiple excitations

Interferences between surface and bulk, extrinsic and intrinsic excitations

Physical parameters and distributions characterizing electron transport in solids

IMFP : inelastic mean free path (*mean free path of electrons for inelastic scattering*)

SEP : surface excitation parameter (*average number of surface excitations at a single surface crossing of an electron*)

TrMFP : transport mean free path ($\lambda_{tr} = (M\sigma_{tr})^{-1}$; $\sigma_{tr} = \int_{4\pi} (1-\cos\theta)(d\sigma/d\Omega)d\Omega$; *M* : *atomic density*; $d\sigma/d\Omega$: *diff. cross section for elastic electron scattering*)

DIIMFP : differential inverse inelastic mean free path

DSEP : differential surface excitation parameter

The IMFP, DIIMFP, SEP and DSEP can be derived from electron backscattering experiments

EAL : effective attenuation length (*a parameter which, when replacing the IMFP in an expression derived from the common AES or XPS formalism (where elastic-electron scattering is neglected) for a given quantitative application, will correct this expression for elastic-scattering effects)*

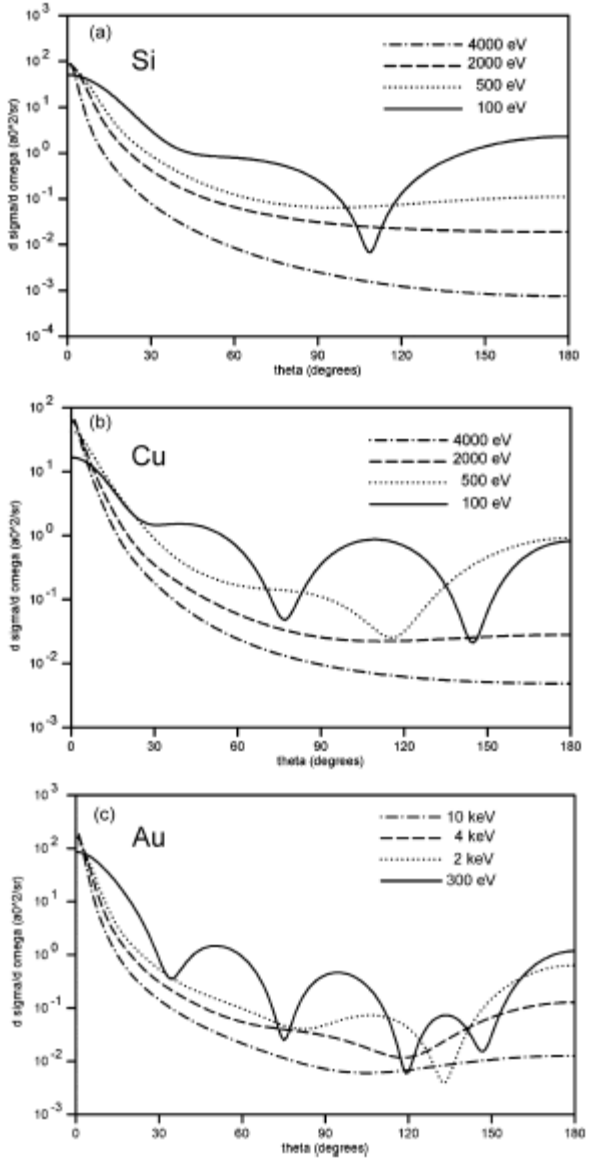

A. Jablonski, F. Salvat, C.J. Powell, NIST Electron Elastic-Scattering Cross Section Database. Version 3.1. Standard Reference Data Program Database 64, U.S. Department of Commerce, National Institute of Standards and Technology, Gaithersburg, MD, 2003, http://www.nist.gov/srd.nist64.htm.

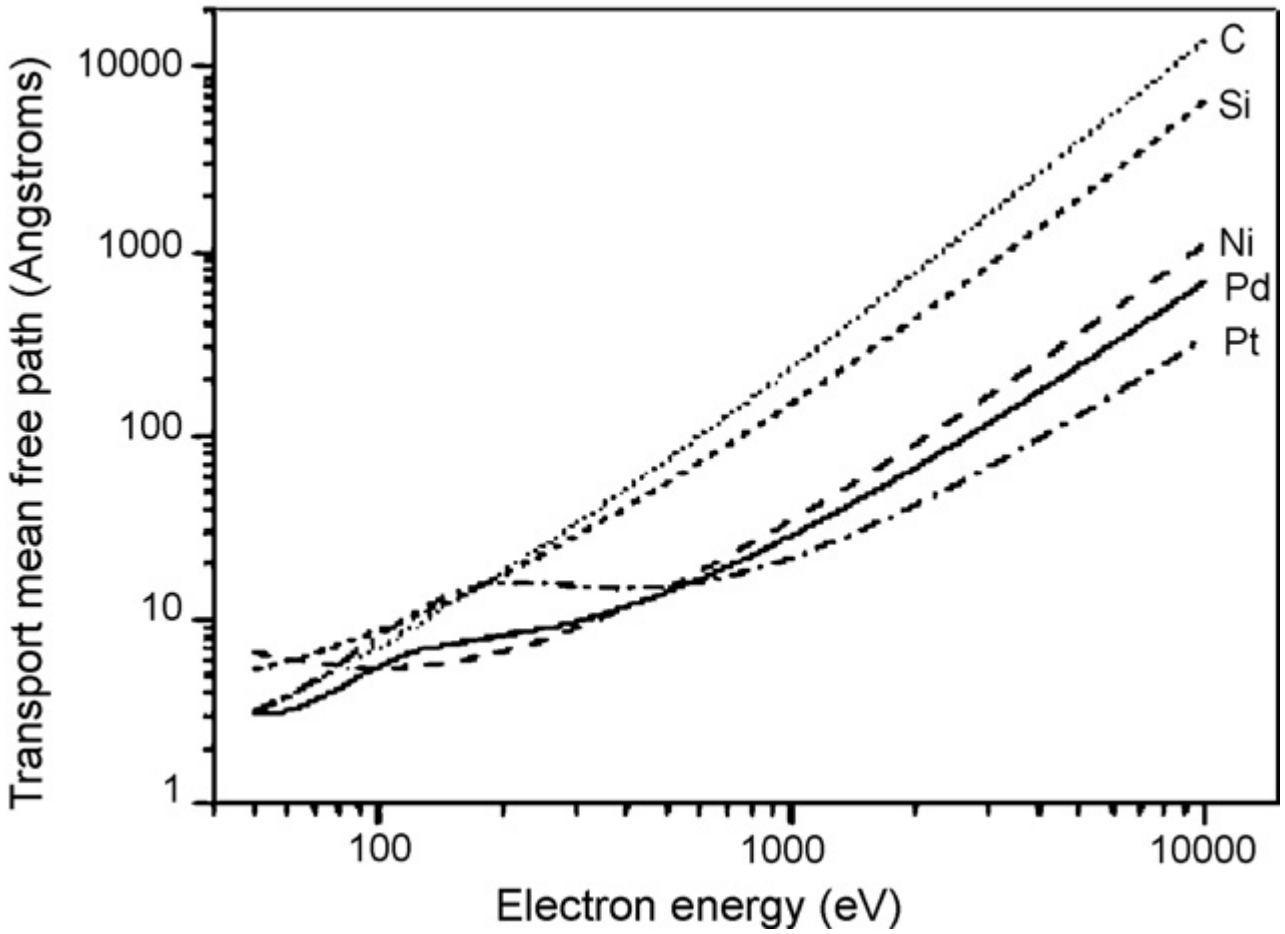

A. Jablonski, Surf. Sci. 603 (2009) 1342

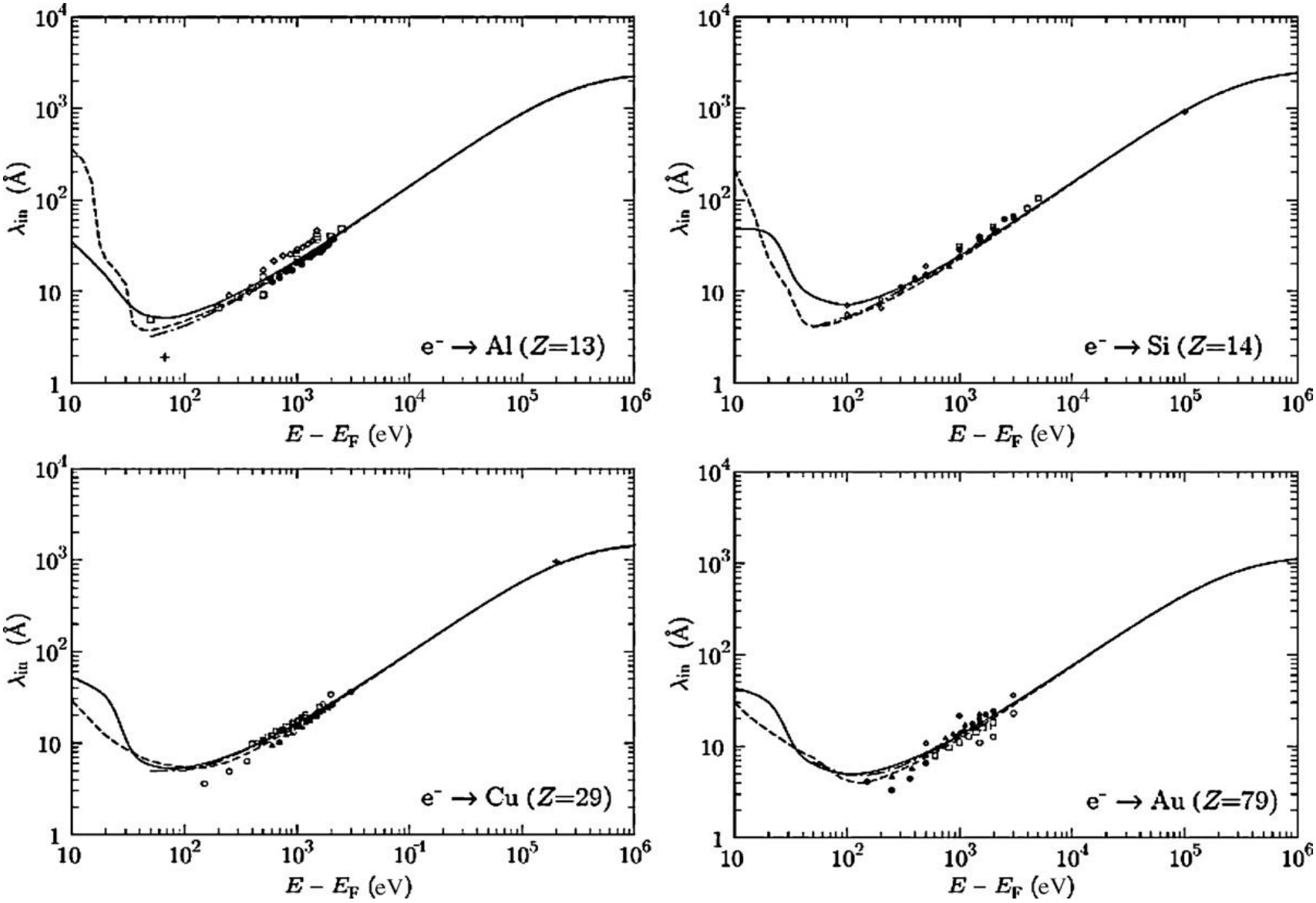

D. Bote, F. Salvat, A. Jablonski, C.J. Powell, J. Electron Spectrosc. Relat. Phenom. 175 (2009) 41

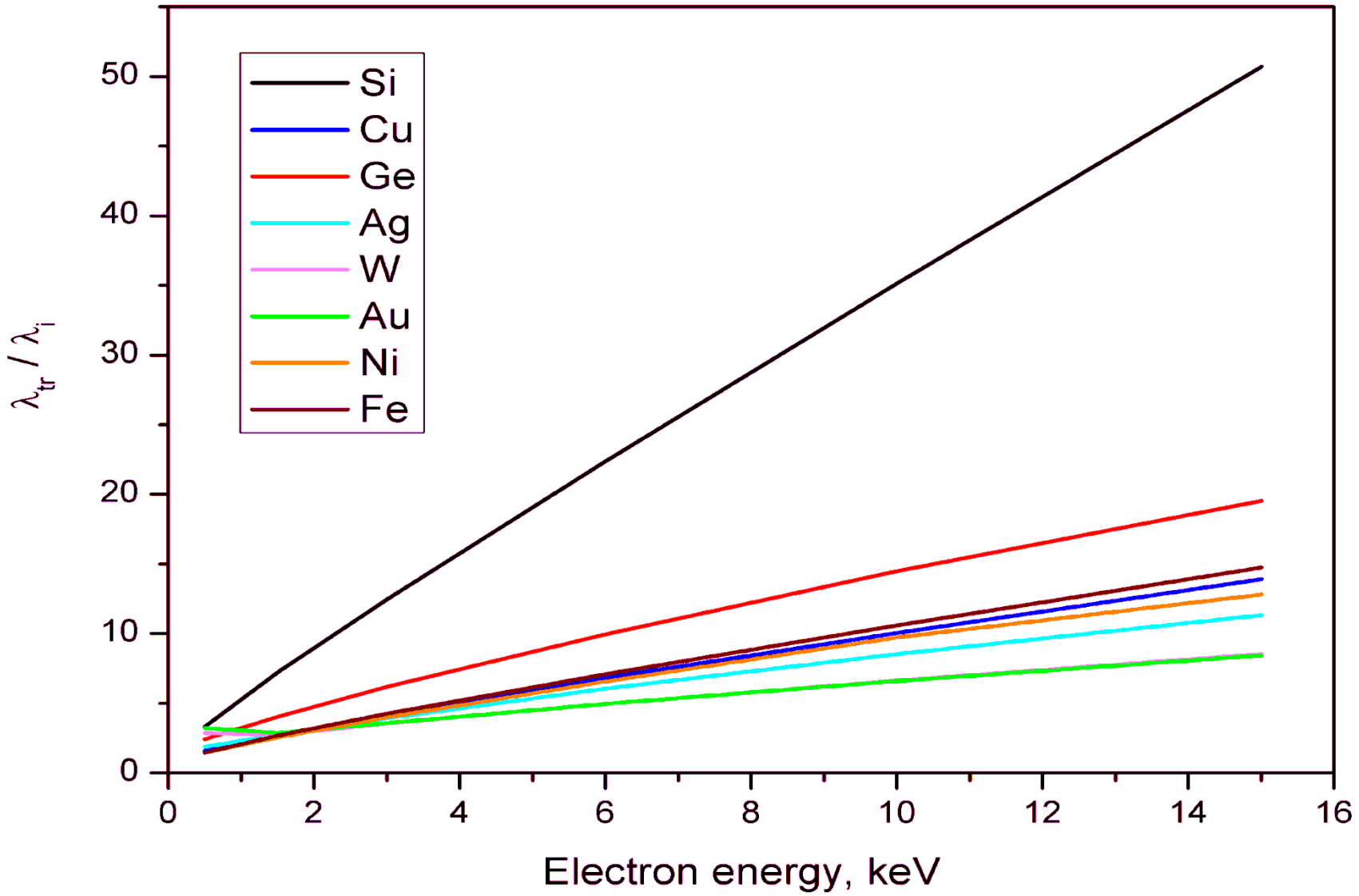

λ_i: TPP-2M, S. Tanuma, C.J. Powell, D.R. Penn, *Surf. Interface Anal.* **21**(1993)165.

$\lambda_{tr} \approx 1/M\sigma_{tr}$: NIST *Electron Elastic Scattering Cross-section Database*, ver. 3.1, 2003.

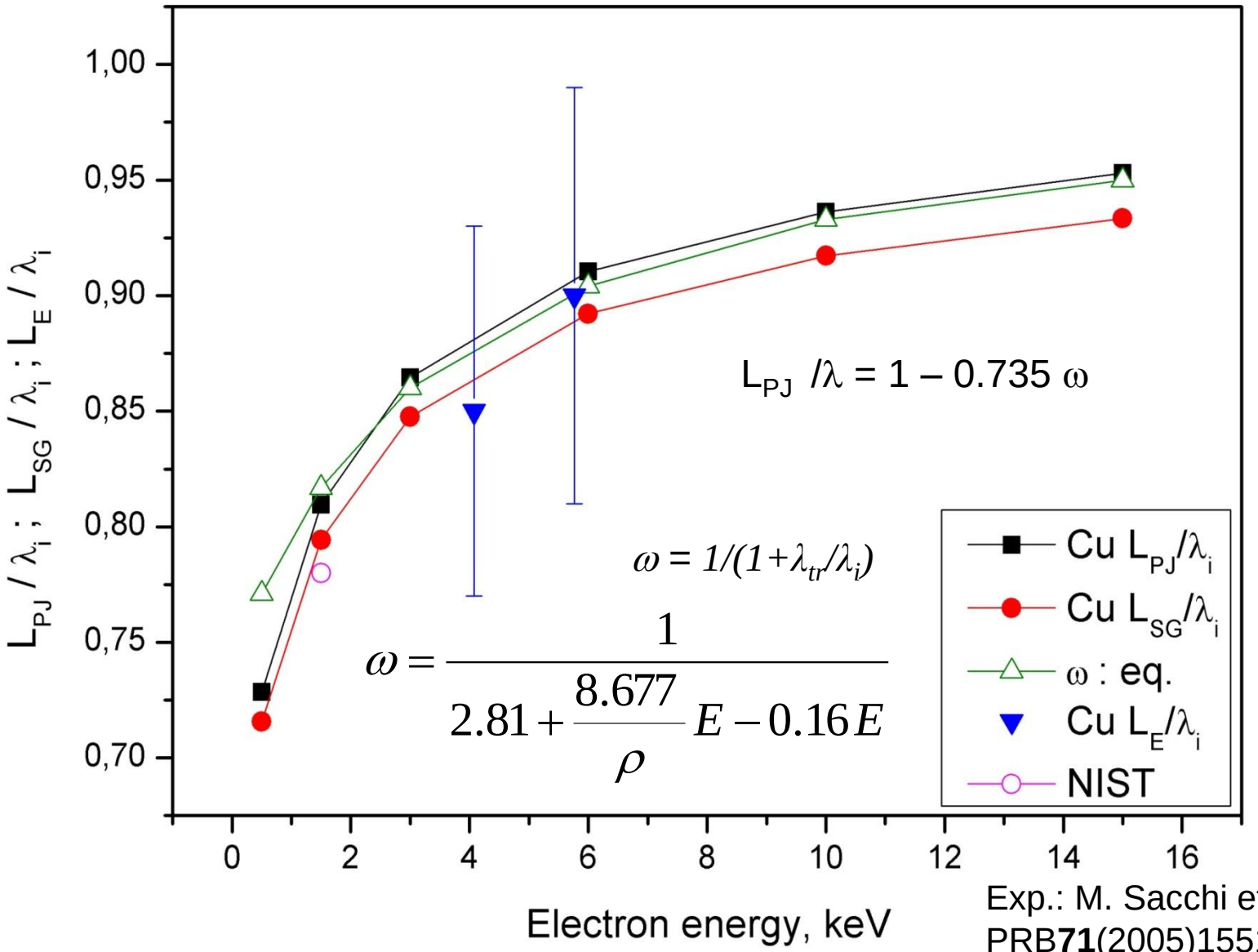

Exp.: M. Sacchi et al., PRB**71**(2005)155117.

NIST : NIST EAL Database, Ver. 1., 2001

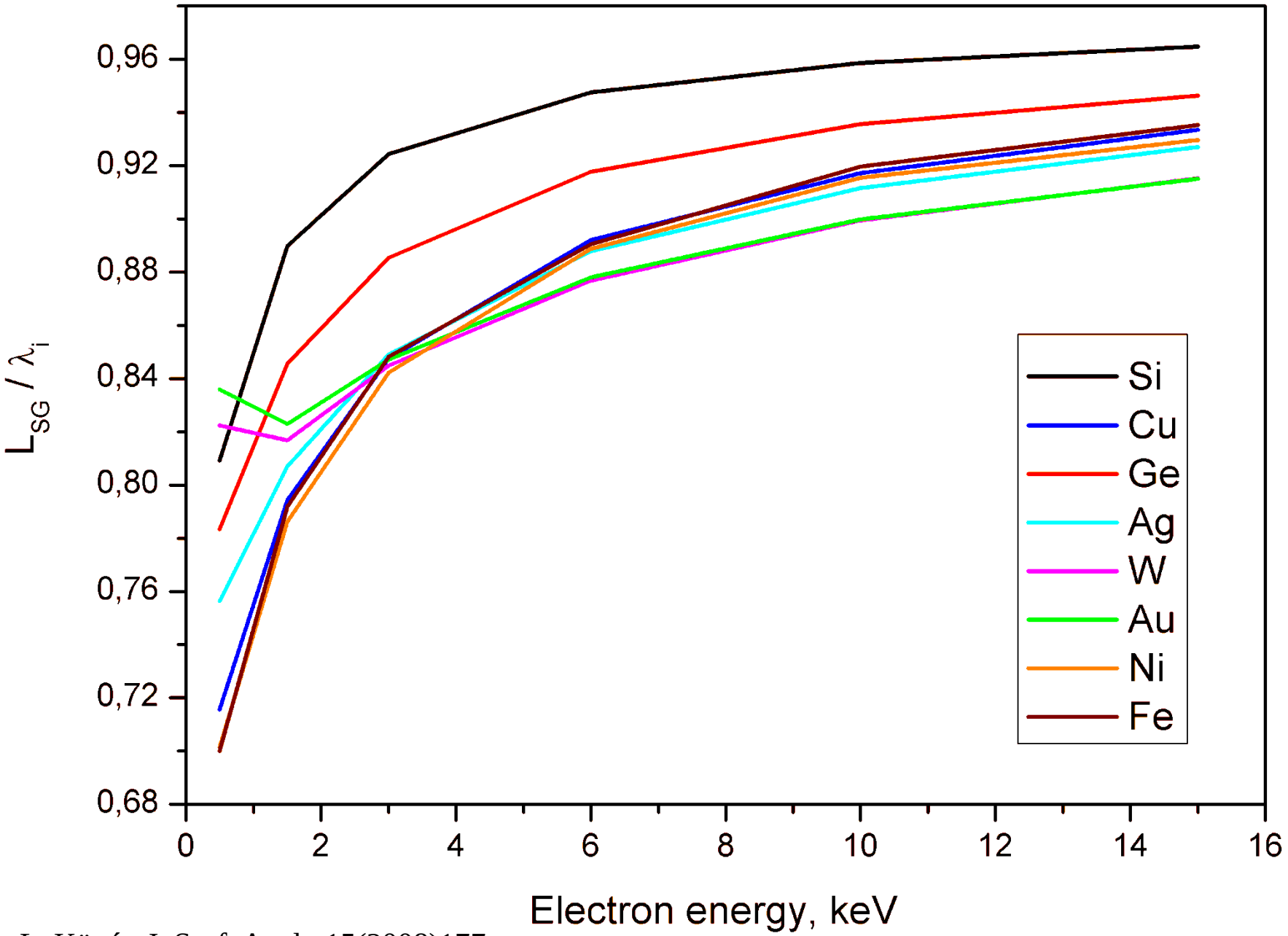

L. Kövér, J. Surf. Anal., 15(2008)177.

A simple method for interpretation of photoelectron lineshapes

The modified Hüfner* model

$$\frac{I_p(n)'}{I_0} = \left(b^n / n!\right) + a\frac{I_p(n-1)'}{I_0} + \left(c^n / n!\right)$$

$I_p(n)'$: intensity of the *n*th plasmon satellite

a, b, c are constants characterizing bulk extrinsic, intrinsic and surface excitations, respectively

DS ⊗ Gaussian primary peak shape

Plasmon peak shape: convolution with energy loss f. derived from optical data and Lindhard's expression (same for bulk extr. & intr.)

Surface energy loss: $\varepsilon \rightarrow (\varepsilon + 1)$ or more accurate approximations

Values for a, b, c from the best fit of the formula to the exp. spectrum

*Hüfner S. in *Photoelectron Spectroscopy* (3rd Edition) Springer, 2003, Chap. 4.

M. Novák, L. Kövér, S. Egri, I. Cserny, J. Tóth, D. Varga, W. Drube, *J. Electron Spectrosc. Relat. Phenom.* **163**(2008)7*;* L. Kövér, M. Novák, S. Egri, I. Cserny, Z. Berényi, J. Tóth, D. Varga, W. Drube, F. Yubero, S. Tougaard, and W.S.M. Werner, *Surf. Interface Anal.* **38**(2006)569.

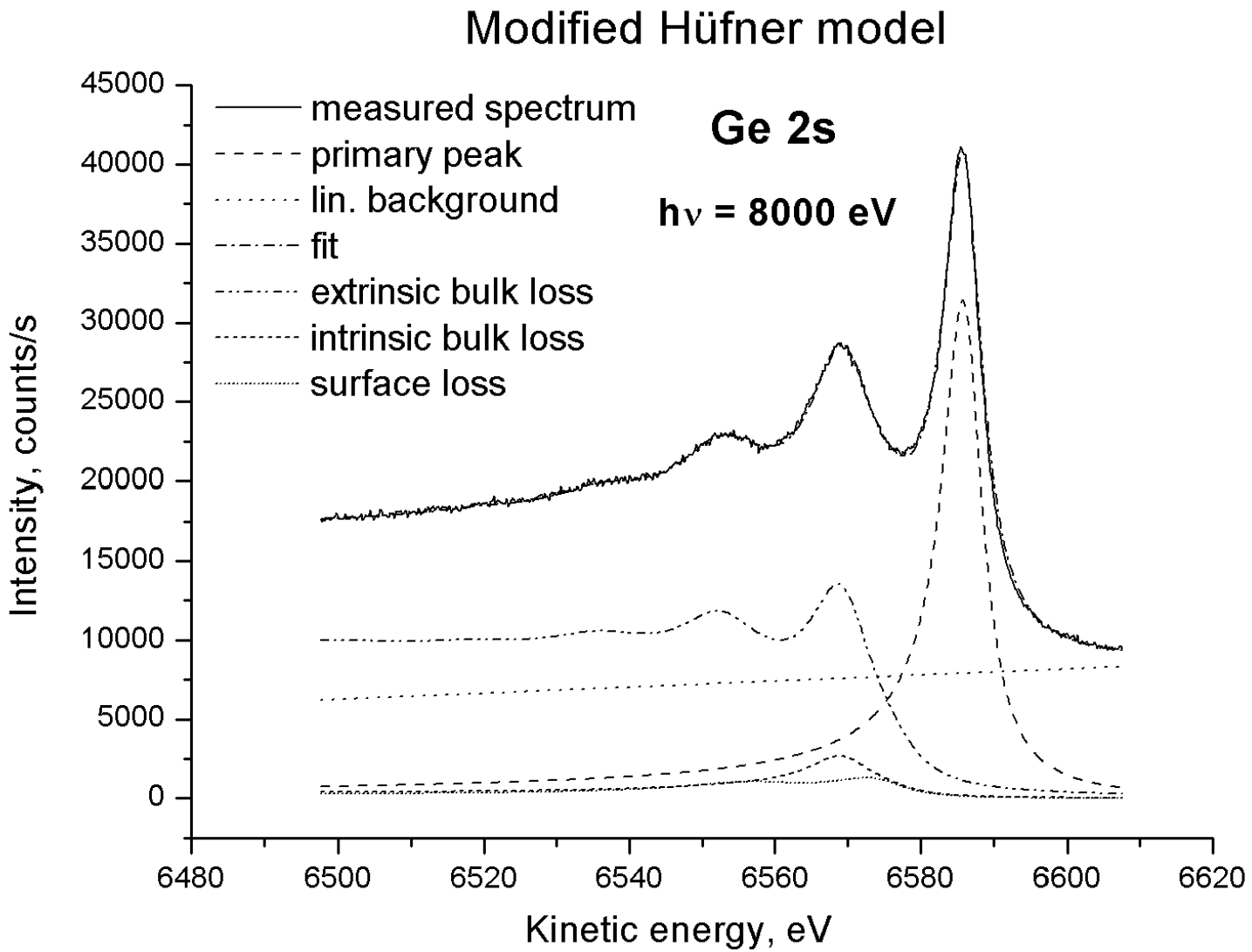

L. Kövér, M. Novák, S. Egri, I. Cserny, Z. Berényi, J. Tóth, D. Varga, W. Drube, F. Yubero, S. Tougaard and W.S.M. Werner, *Surf. Interface Anal.* **38**(2006)569.

XPS dielectric response model

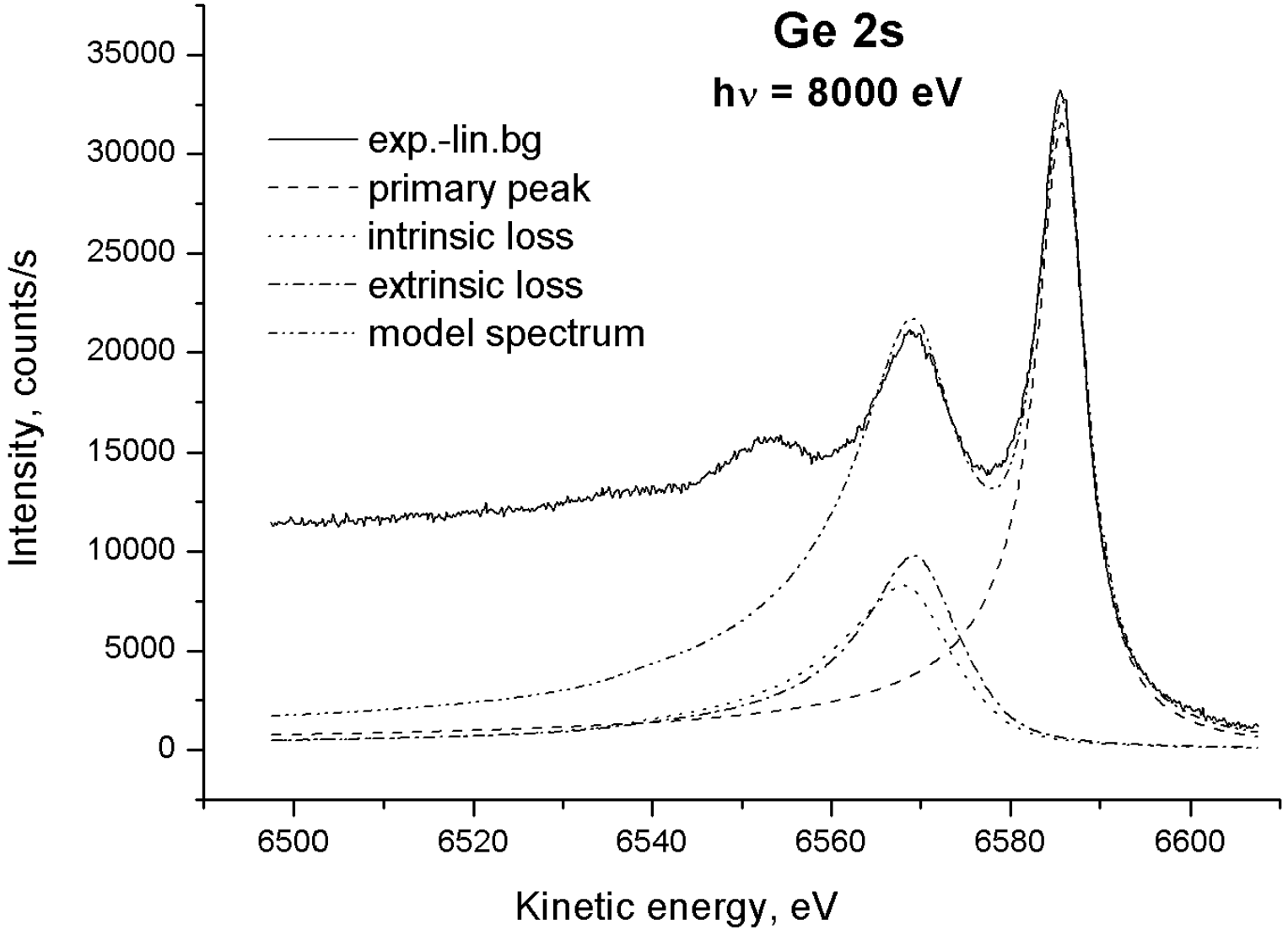

L. Kövér, M. Novák, S. Egri, I. Cserny, Z. Berényi, J. Tóth, D. Varga, W. Drube, F. Yubero, S. Tougaard and W.S.M. Werner, *Surf. Interface Anal.* **38**(2006)569.

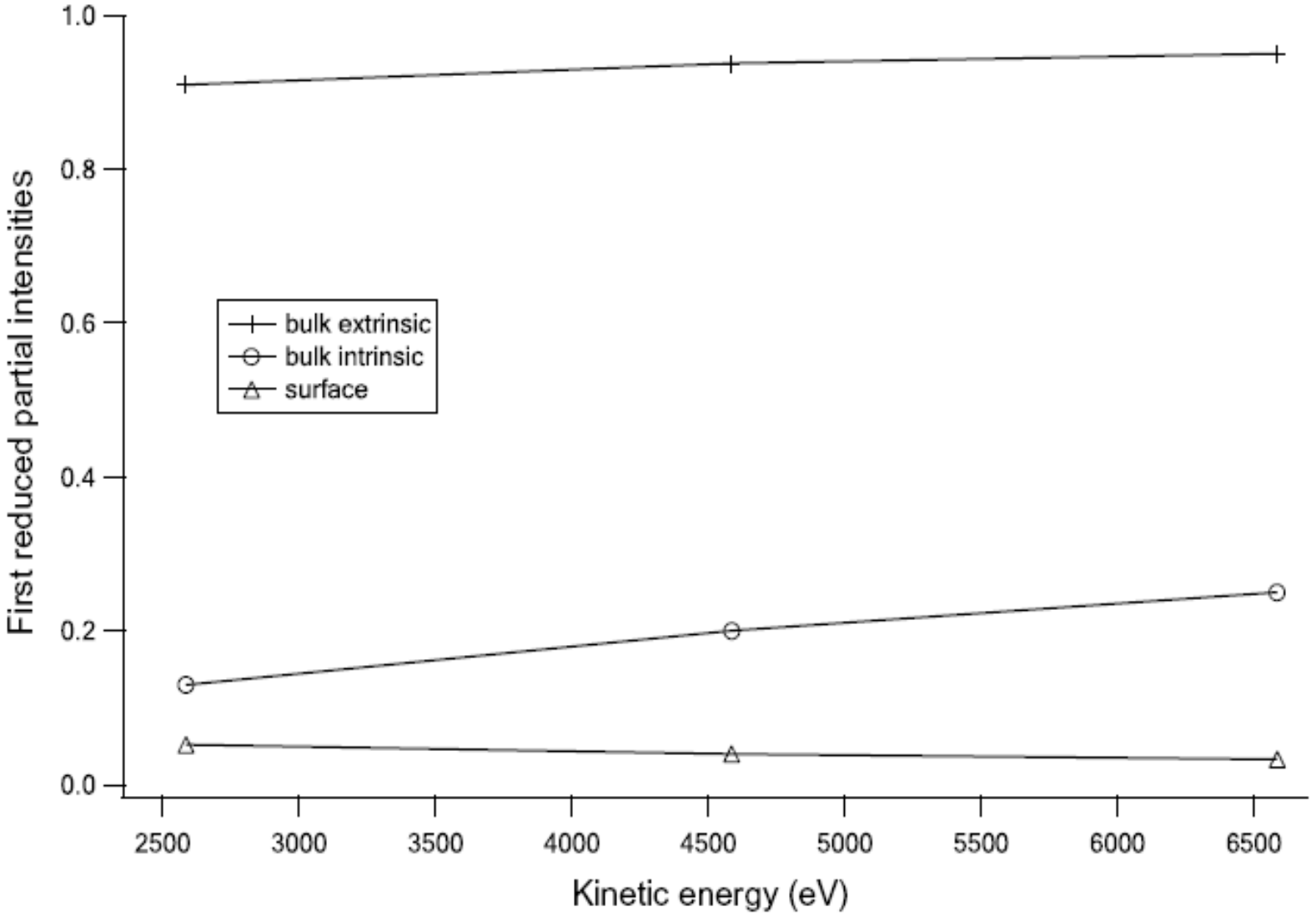

M. Novák, S. Egri, L. Kövér, I. Cserny, W. Drube, W. S. M. Werner, Surf. Sci., **601**(2007)2344.

Si 1s

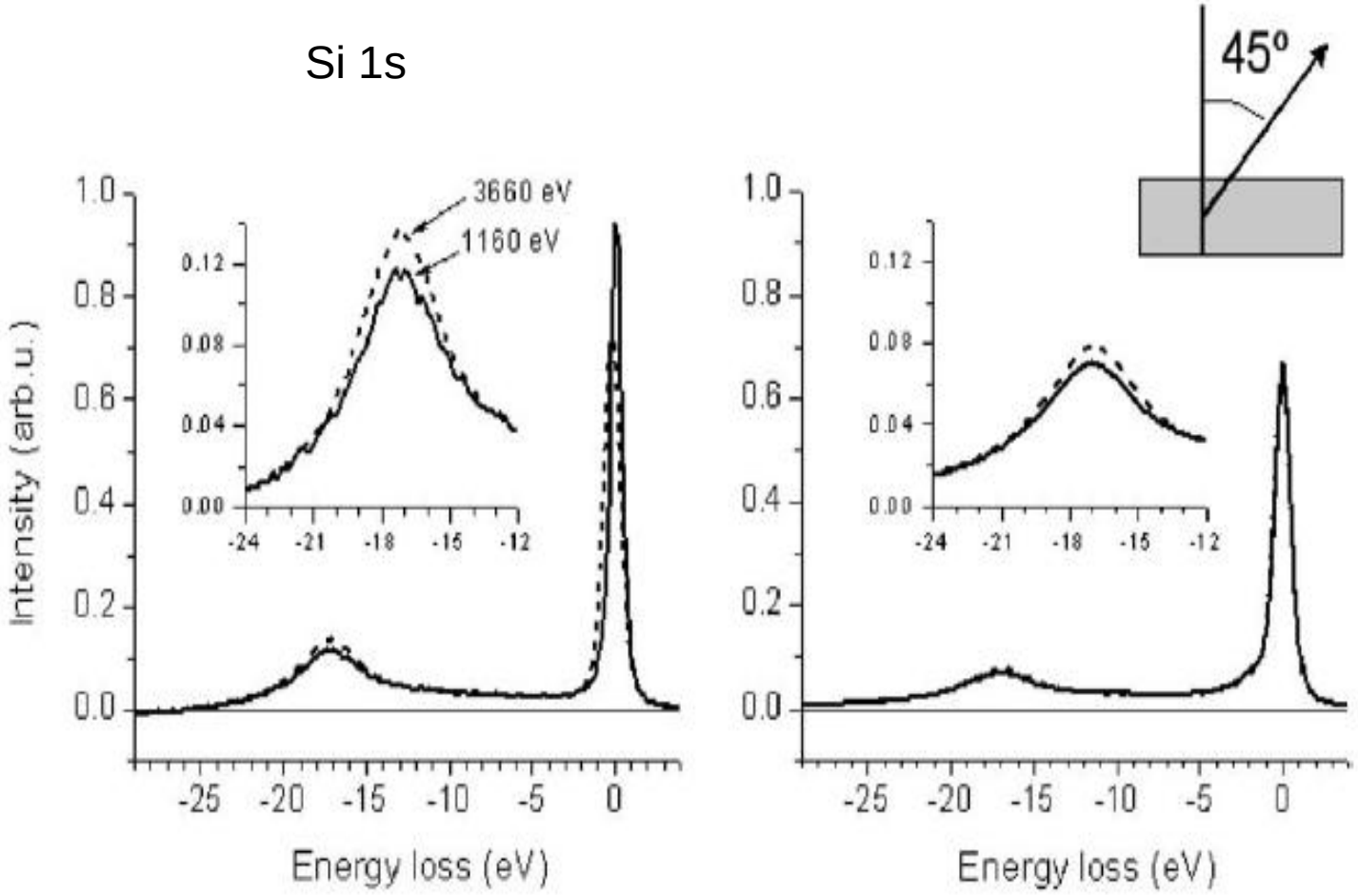

F. Yubero, L. Kövér, W. Drube, Th. Eickhoff, S. Tougaard, Surface Sci. 592(2005)1.

Interference between intrinsic and extrinsic bulk excitations

Langreth-model (J. J. Chang, D. C. Langreth, Phys. Rev. **B8**(1973)4633):

$$I_p/I_0 = a^n \sum^n_{m=0} (b/a)^m/m! \qquad P_{int} = e^{-b} b^n/n!$$

I_p : bulk plasmon intensity; I_0 = intensity of the main peak;
P_{int} = probability of the intrinsic excitation

Fast-slow interference term: $b \rightarrow b - (e^2/\hbar v)\chi$;
where v is the electron velocity, χ varies slowly with v, ~ the product of extrinsic and intrinsic plasmon excitation probabilities

Nearly free electron model, modified Langreth equation (Biswas et al., Phys. Rev. **B**67(2003)165416) :

$$I_p/I_0 = a^n \sum^n_{m=0} [(b- (e^2/\hbar v)\chi)/a]^m/m!$$

Interference term $-(e^2/\hbar v)\chi$: *always negative*
decreases for high n
vanishes at very high electron kinetic energies

Estimation of parameters *a, b, c,* characterizing the probabilities of extrinsic, intrinsic bulk and surface excitations

c → SEP (Poisson distribution), can be calculated using dielectric models or derived experimentally

a → κ (assumption: exponential distribution) e. g. :

$$\kappa = 1 - (\omega/2(1 + \cos\theta\,(3(1 - \omega))^{1/2}\,)$$

where θ is the polar angle of detection, related to the surface normal
(I. S. Tilinin, W. S. M. Werner, *Surf. Sci.* **290**(1993)119.)

b → ????? (Poisson distribution) $b \sim 0.12\, r_s$, $r_s \sim (47.11/\hbar\omega_p)^{2/3}$
$\hbar\omega_p$ *:* bulk plasmon energy
(W. J. Pardee et al. PRB **11**(1975)3614; D. C. Langreth, PRL **26**(1971)1229.)

Calculations of ***a*** and ***b*** using dielectric response models (directly) or indirect derivations from fitting experimental spectra to model spectra (PIA, MH)

Intrinsic surface excitations ??? Interference terms ???

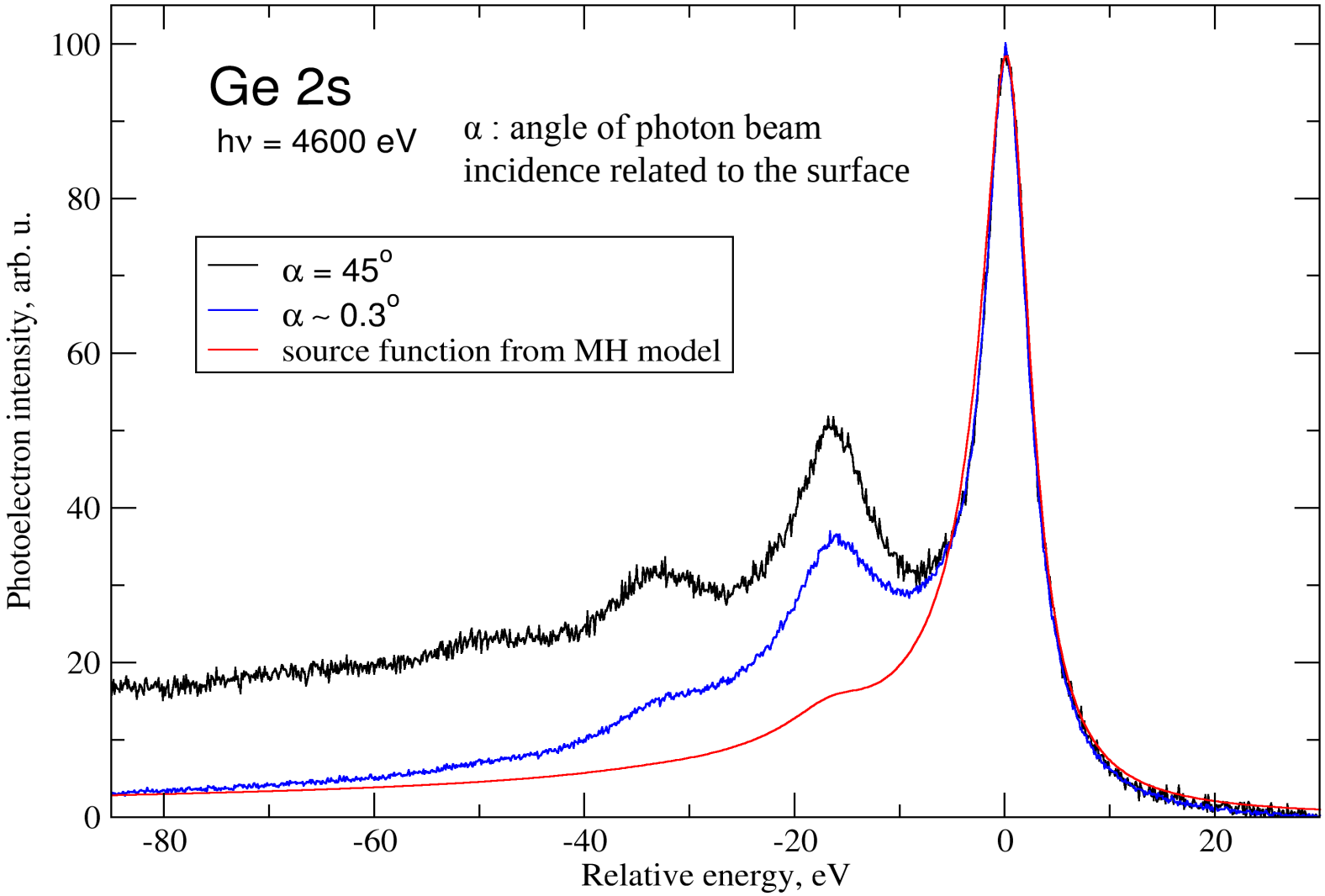

Kövér L., Cserny I., Novák M., Egri S., HASYLAB Annual Report 2007 (2007)1591.

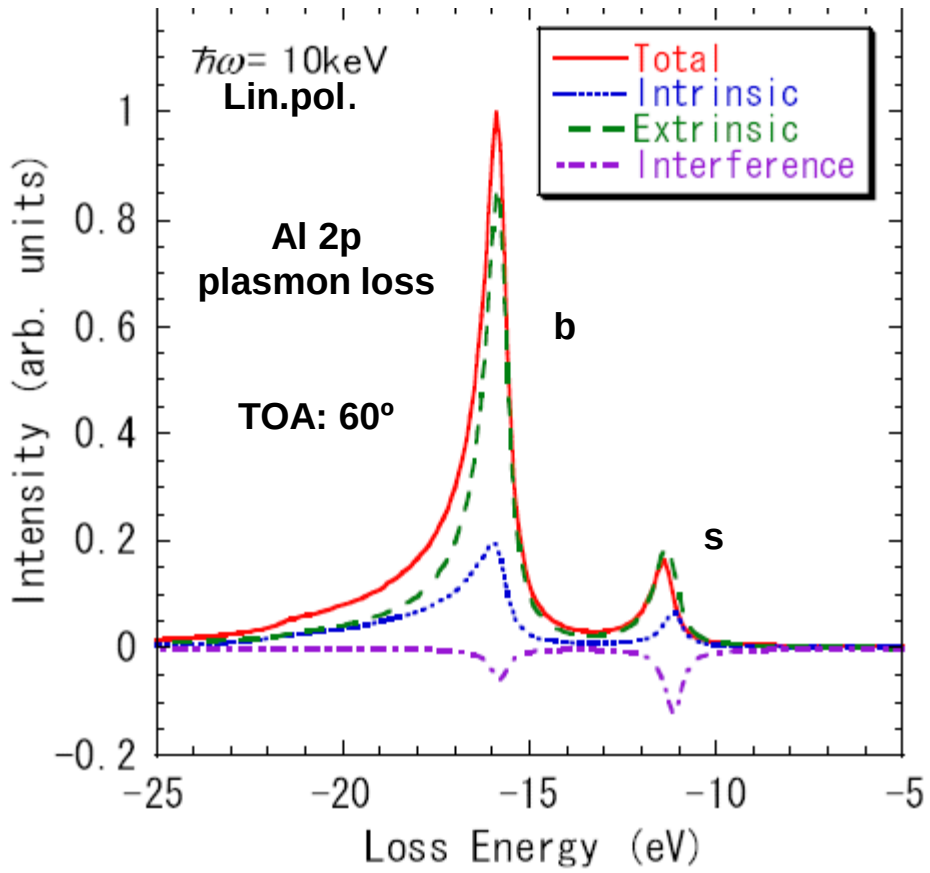

T. Fujikawa et al., e-J. Surf. Nanotech. 6(2008)263.

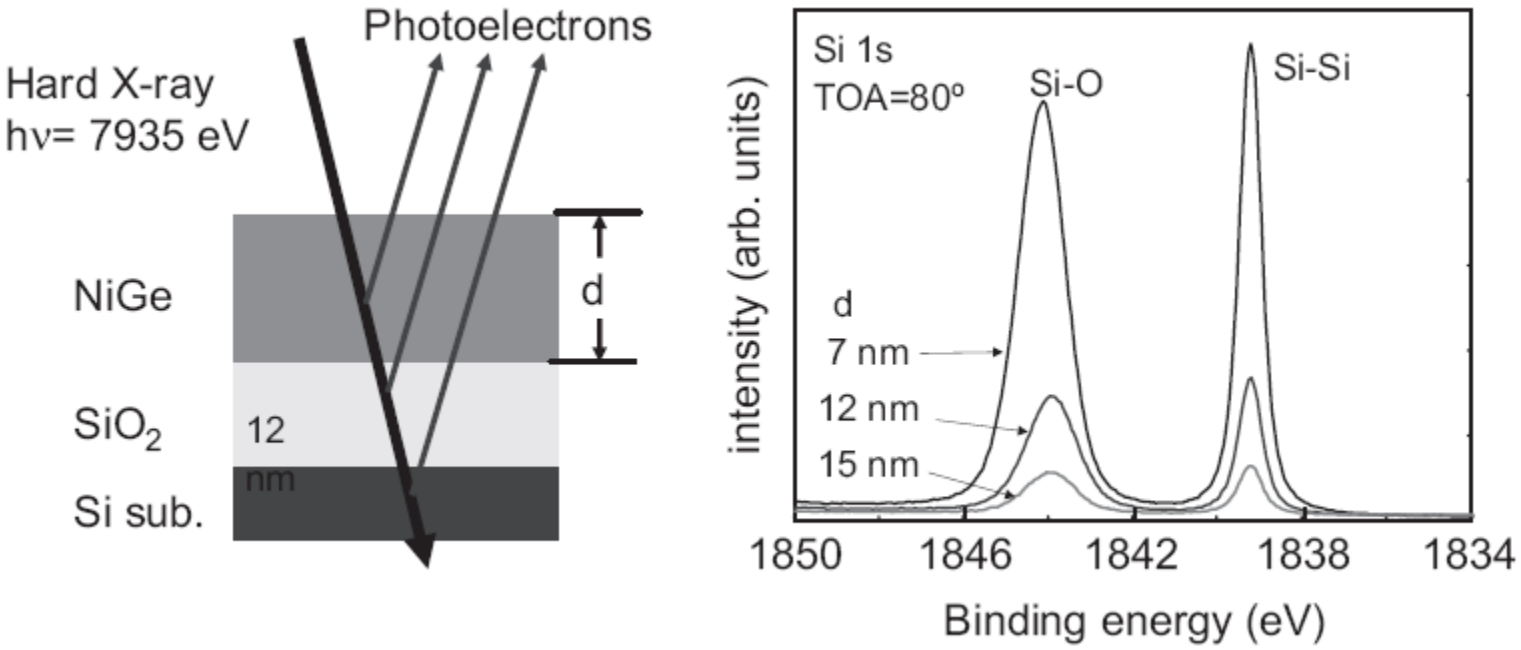

K. Kobayashi, Nucl. Instrum. Meth. A 601(2009)32.

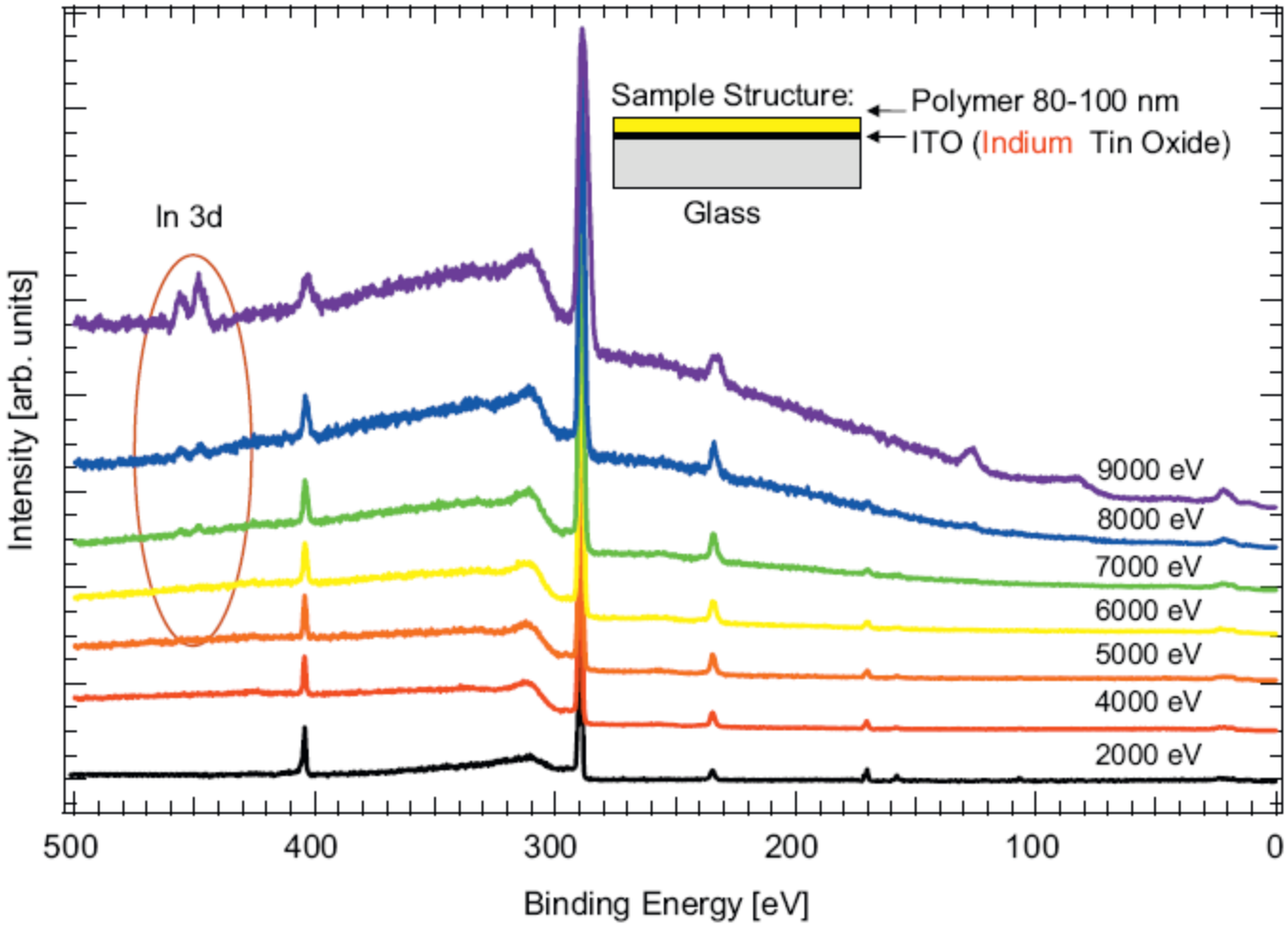

M. Gorgoi et al. Nucl. Instrum. Meth. Phys. Res. A 601(2009)48.

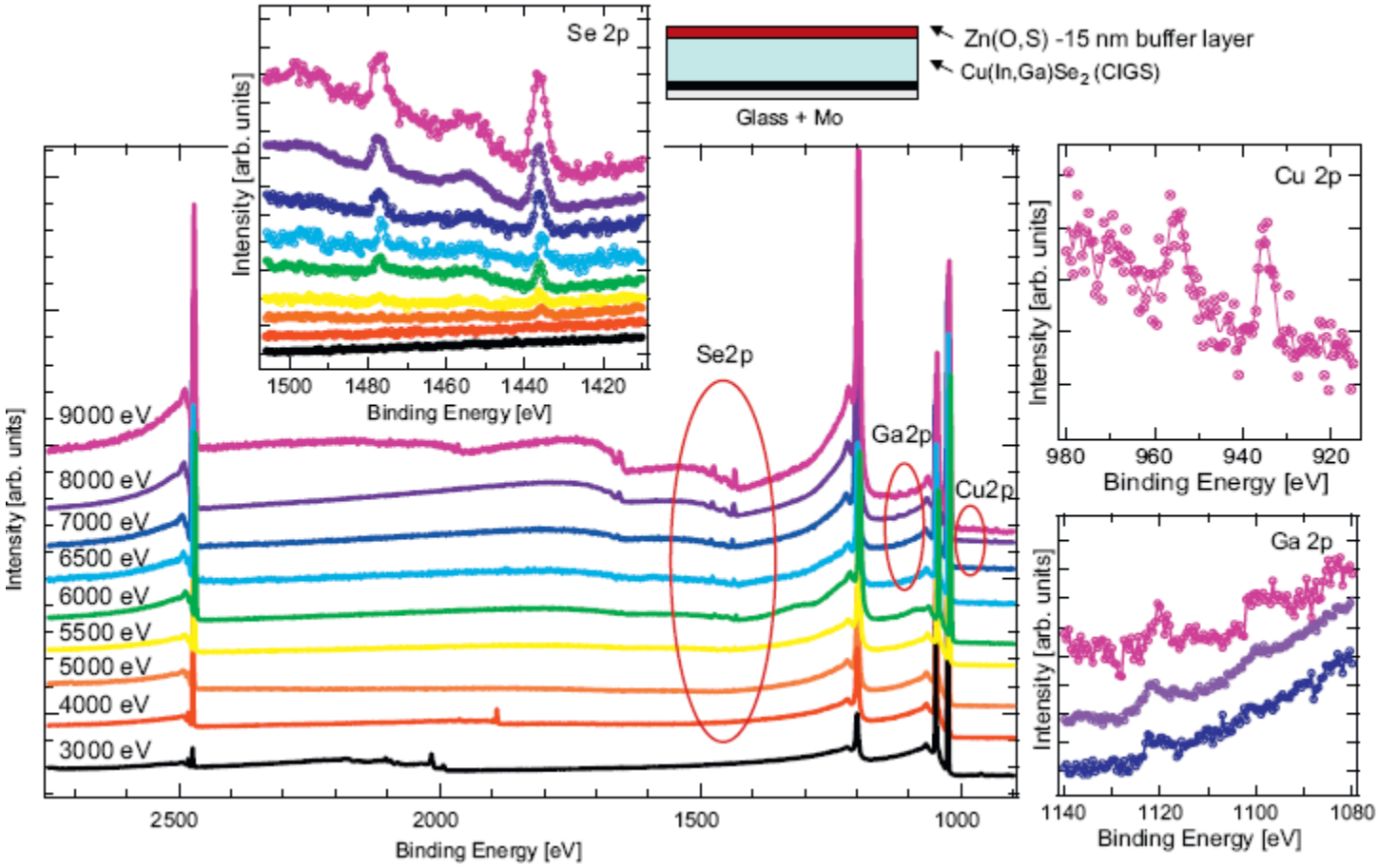

M. Gorgoi et al., Nucl. Instrum. Meth. Phys. Res. A601(2009)48.

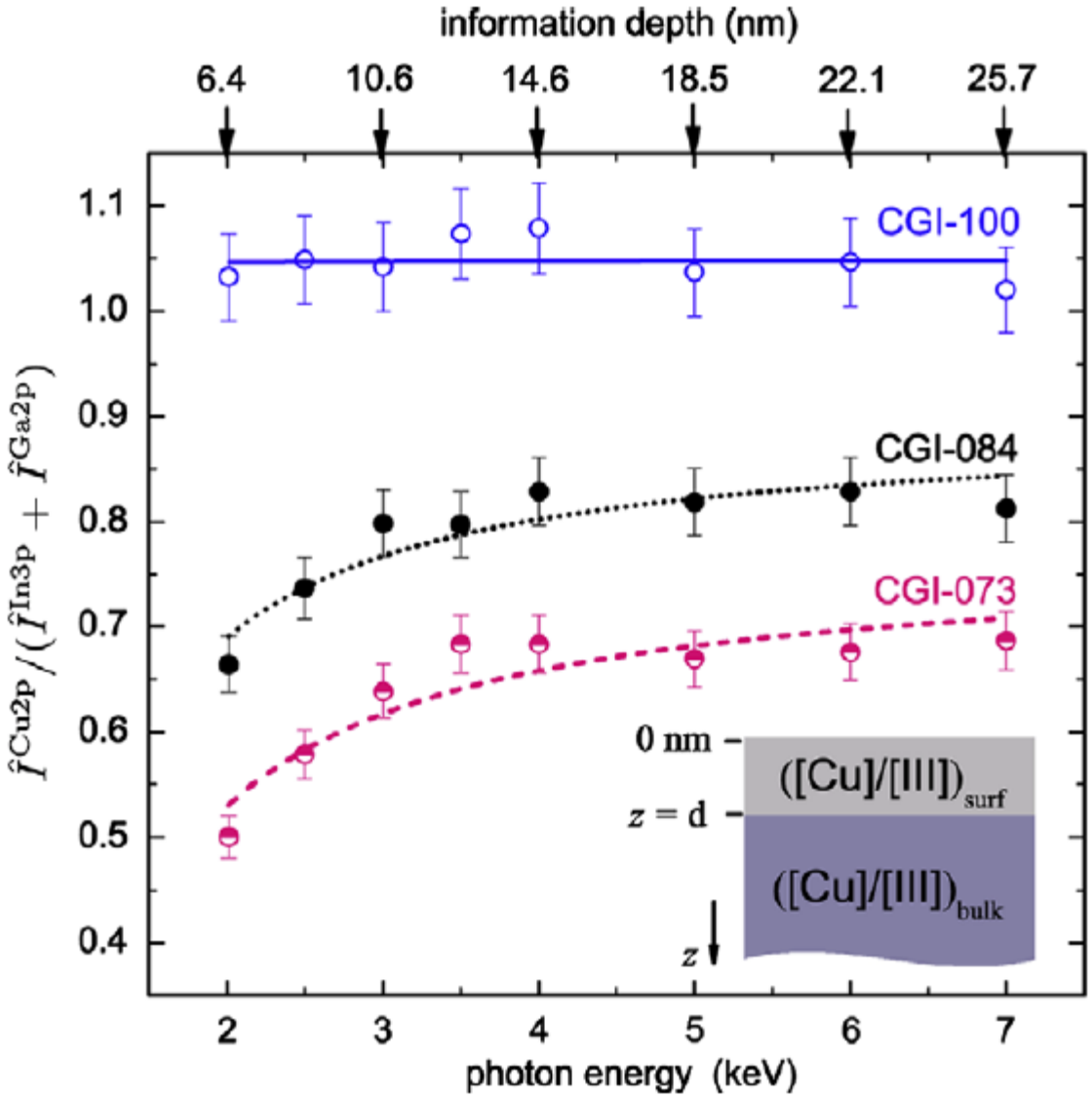

([Cu]/[III])$_{int}$		([Ga]/[III])$_{int}$	Sample name
As grown	KCN etched	As grown/KCN	
1.00	0.91	0.32	**CGI-100**
0.84	0.82	0.28	**CGI-084**
0.73	0.75	0.39	**CGI-073**

H. Mönig et al., Acta Materiala 57(2009)3645.

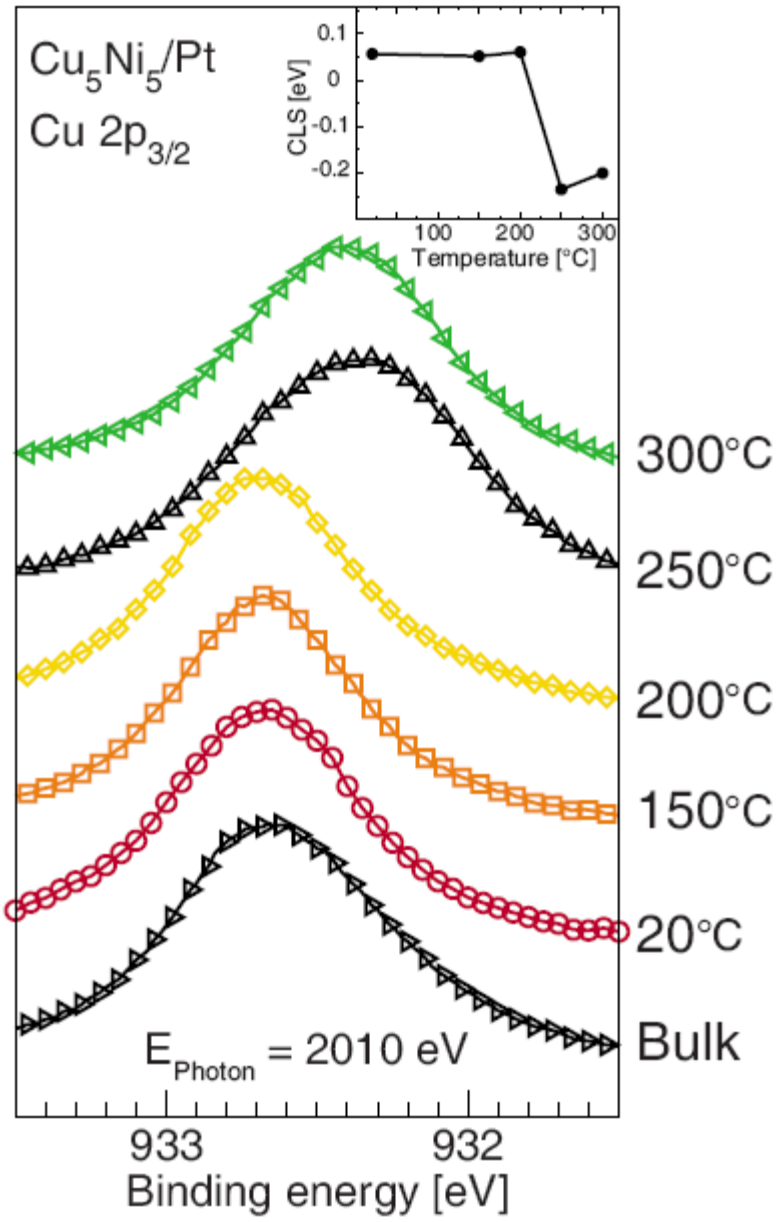

S. Granroth et al., PRB 80(2009)094104

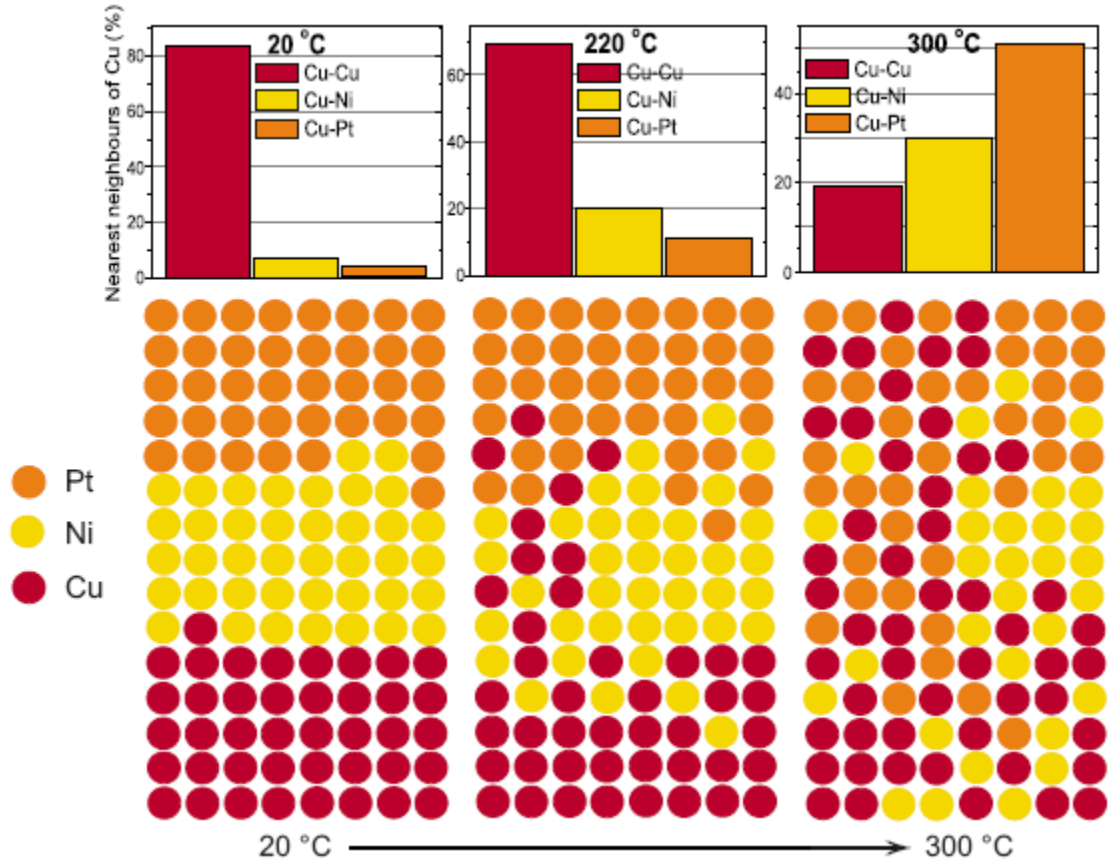

S. Granroth et al., PRB 80(2009)094104

Determination of concentration depth profiles (CDP) using varying kinetic energy XPS (ERXPS)

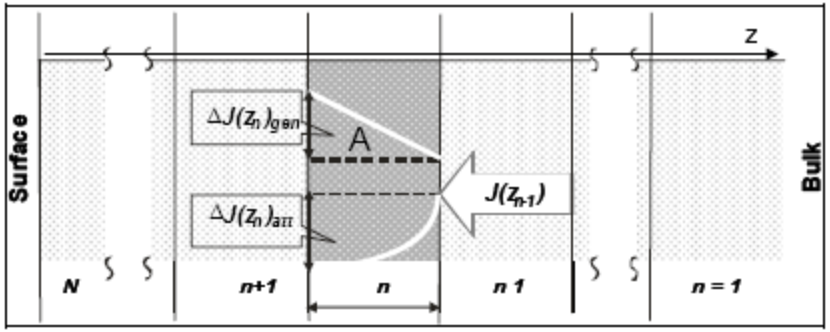

„Infinitesimal layer model"

$$J_A(z_n) = \sigma_A \rho_A(z_n)\Delta z + J_A(z_{n-1})\exp(-\Delta z/\lambda(z_n))$$

$$\lambda(z_n) = \sum_j x_j(z_n)\lambda_j(E_{\mathrm{kin},k}) \qquad x_j = \rho_j(z_n)/\sum \rho_j(z_n)$$

$$P_k = \left(\frac{I_B}{I_A}\right)_k \approx \left(\frac{J_{B,z_N}(\rho_B)}{J_{A,z_N}(\rho_A)}\right)_{hv_k}$$

Different functions can be selected for CDPs, the parameters of these functions are determined.

S. V. Merzlikin et al., Surf. Sci. 602(2007)755; S. V. Merzlikin, PhD Theses (2007), Ruhr Univ. Bochum; „DepthProfile" software (N.N. Tolkachev)

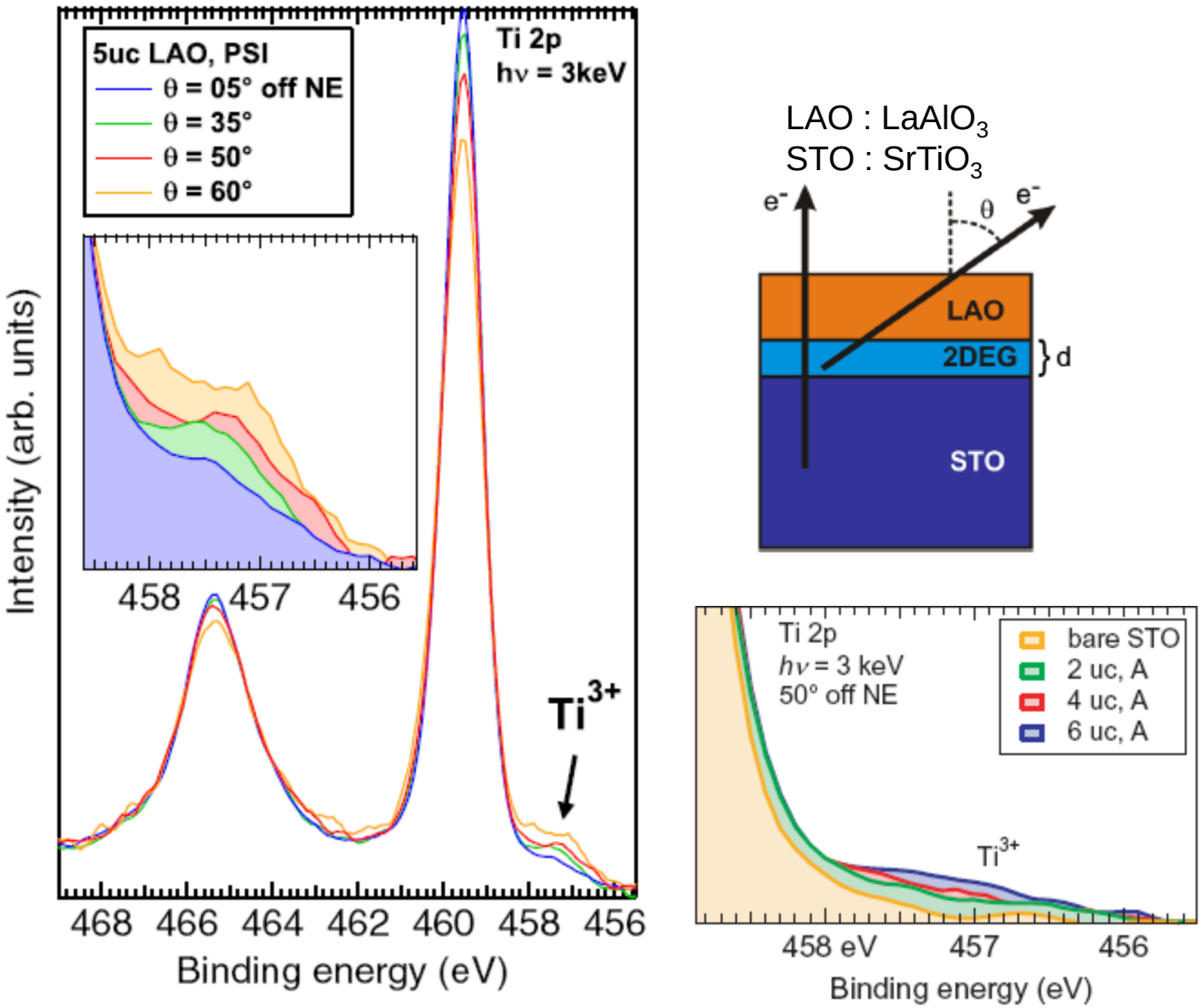

M. Sing et al., Phys. Rev. Lett. 102(2009)176805.; R. Claessen et al., New J. Phys. 11(2009)125007.

Summary and perspectives

- ***Elastic electron scattering and surface excitations have strongly decreasing role*** at higher electron energies (EAL→IMFP).
- ***Non-dipole effects*** in HAXPES result in ***significant changes in the angular distribution*** of photoelectrons.
- ***Interferences between bulk intrinsic and extrinsic excitations are expected to decrease with increasing photoelectron energy***: the accuracy of approximations based on the separation of intrinsic and extrinsic processes is expected to improve.
- The possible ***role of intrinsic excitations and interference effects in the case of Ge 2s, Fe 1s and Al 2p*** photoelectron spectra excited from solids has been demonstrated.
- ***Nondestructive quantitative chemical analysis (or concentration depth profiling) of deeply buried interface layers*** has become feasible through the angle resolved HAXPES or varying the excitation energy.
- The examples illustrating the capability of the hard X-ray photoelectron spectroscopy for revealing details of chemical composition of deeply buried interfaces as well as of bulk electronic structure, together with the new instrumental developments and the important information from high energy REELS **confirm the expectations for the further and quick increase of the power of this method.**

Acknowledgements

The research leading to these results has received funding from the European Community's Seventh Framework Programme (FP7/2007-2013) under grant agreement n° 226716. The support of the Hungarian grant OTKA K67873 is gratefully acknowledged.

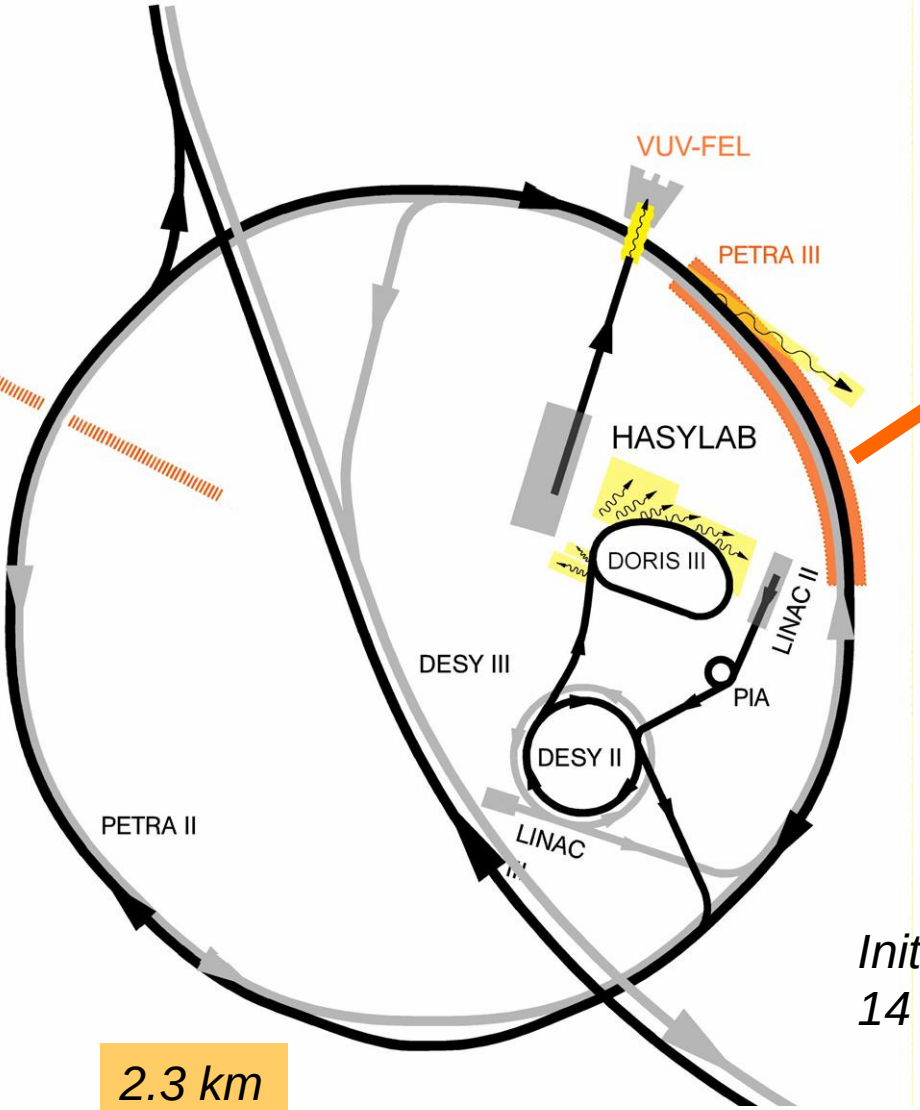

2.3 km

6 GeV / 100 mA (200 mA)
1 nmrad emittance
top-up mode operation

Currently the most brilliant
hard X-ray storage ring source

Initial phase:
14 undulator beamlines, ~ 20 end stations

including a HAXPES instrument !

Schematic beamline layout

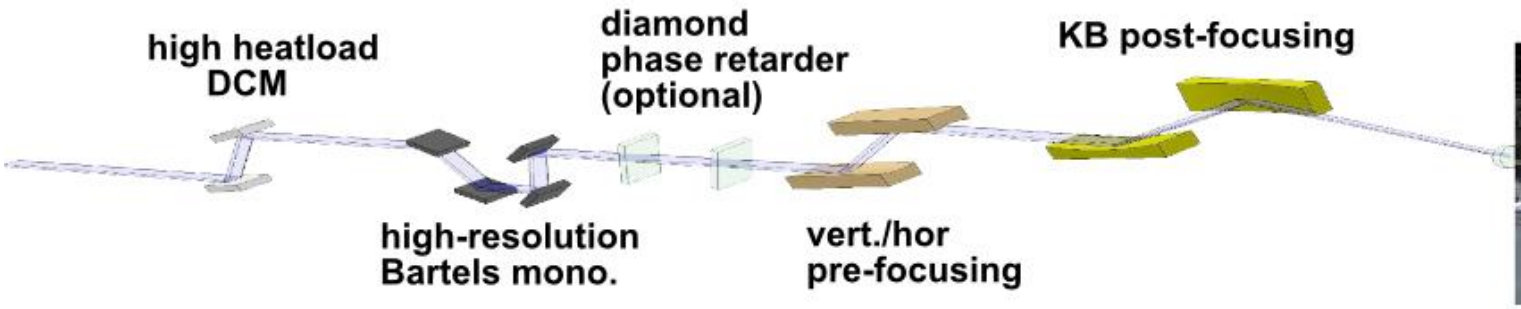

SPECS Phoibos 225
electron analyzer

Photons:

spectroscopy undulator 2.4 - 30 keV
variable circular + linear polarization (phase retarder)
high-res. 4-crystal post-mono (down to 10 meV)
95 m source to sample distance
KB focus down to ~ 1µm x 1µm

Electrons:

SPECS Phoibos 225 analyzer (max. 15 keV)
resolution down to < 50 meV (at ~10-15 keV)

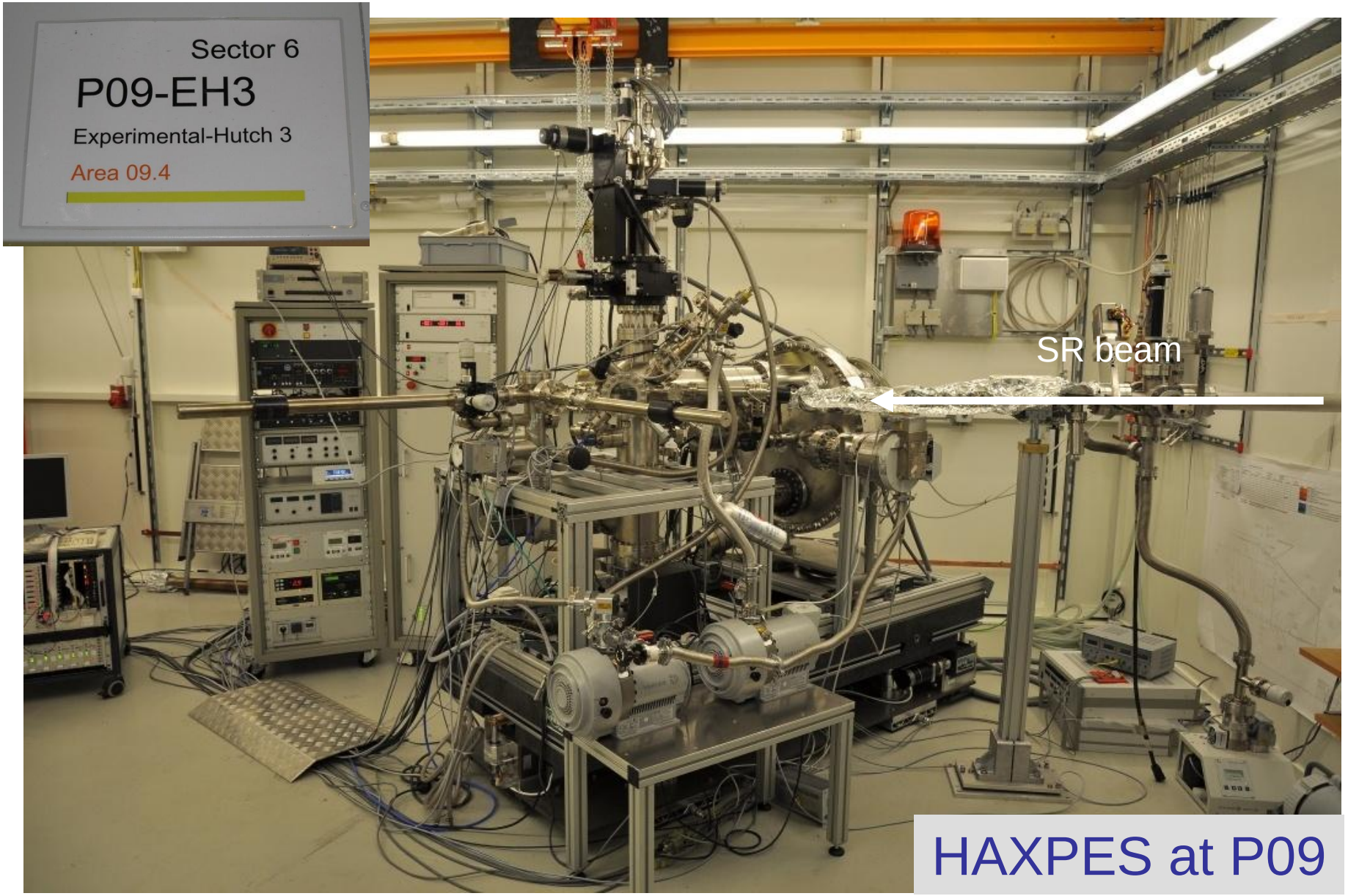

HAXPES at P09

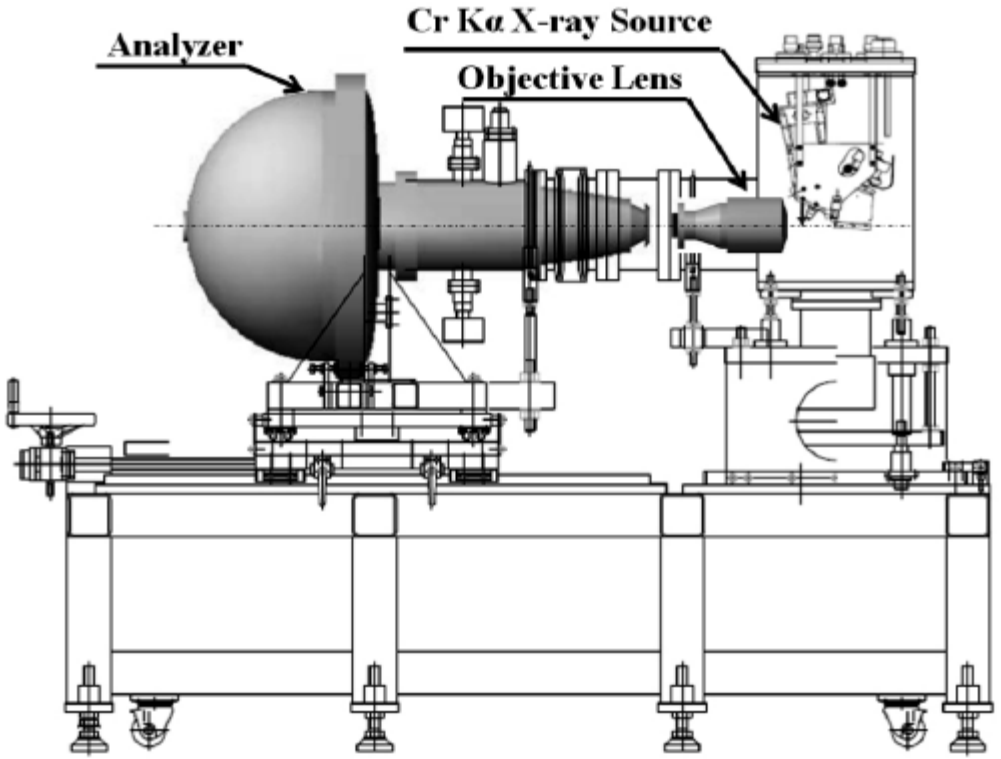

Fig. 1 Schematic view of laboratory HXPS combined with the wide acceptance angle objective lens, monochromatic Cr K_α X-rays, and VG Scienta R4000 10 kV analyzer.

M. Kobata et al., Analytical Sciences (Japan) 26(2010)227

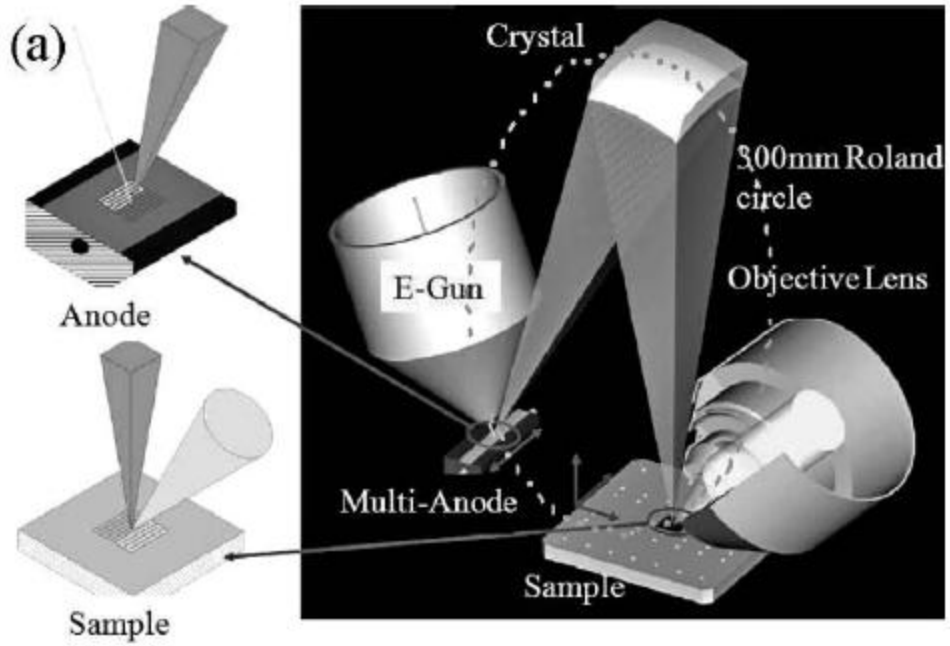

M. Kobata et al., Analytical Sciences (Japan) 26(2010)227

(b) ***Scanning X-ray SED Image***

Sample: Cu Mesh 300LPI

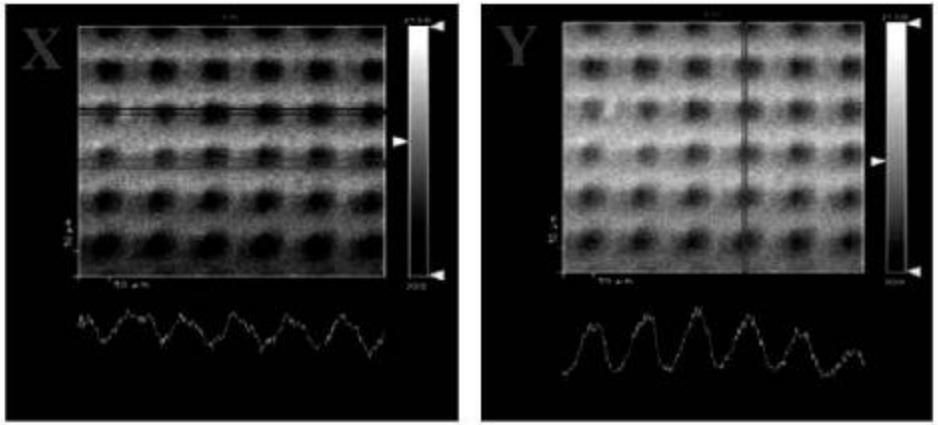

Spatial Resolution

X: *9.11 μm* Y: *8.37 μm*

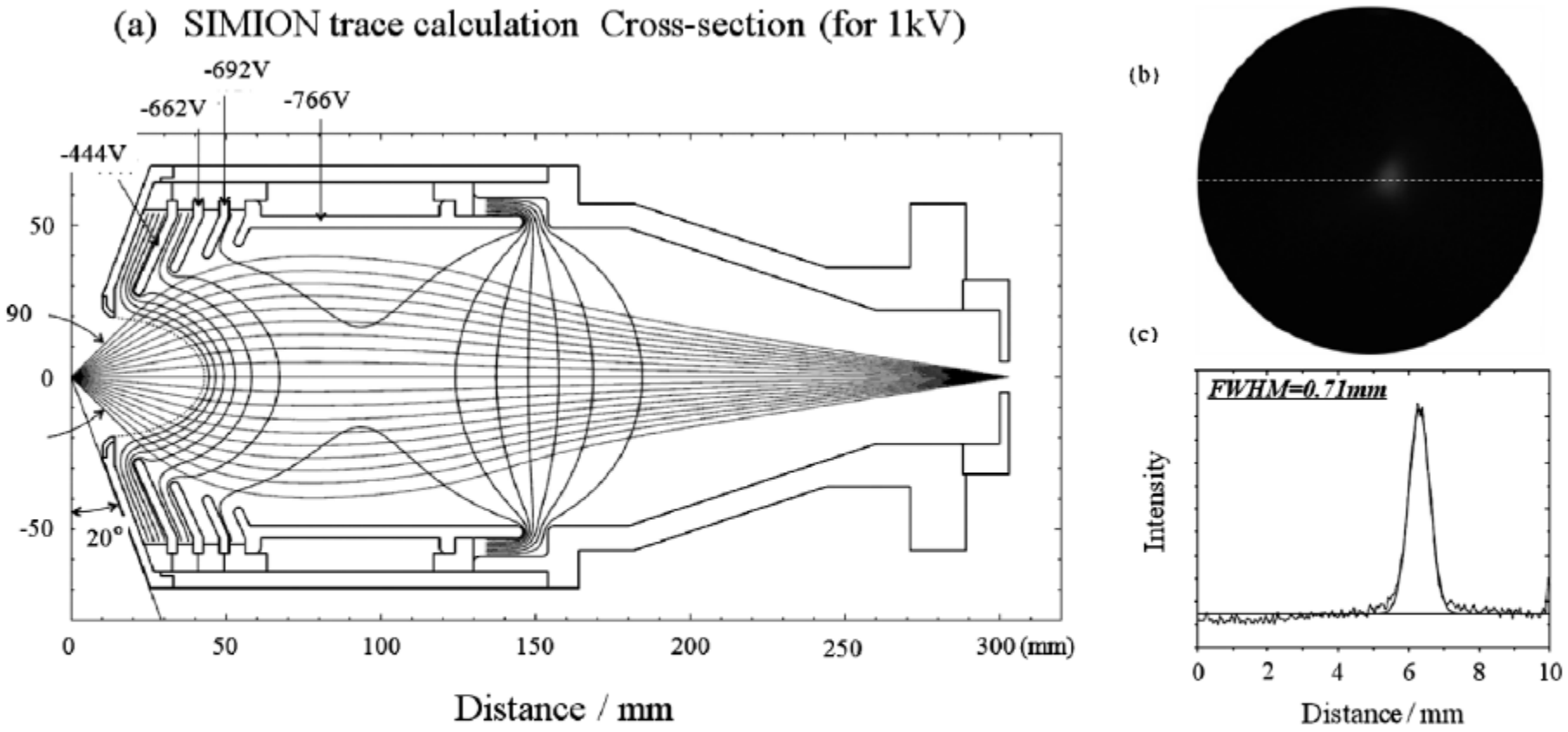

Fig. 3 (a) Structure and electron trajectory simulation of the wide acceptance objective lens. (b) Focused spot at the exit of the wide acceptance objective lens. (c) Cross-section profile of the focused spot (Profile of the image along the line indicated in (b)).

M. Kobata et al., Analytical Sciences (Japan) 26(2010)227; Tóth L. 2008.

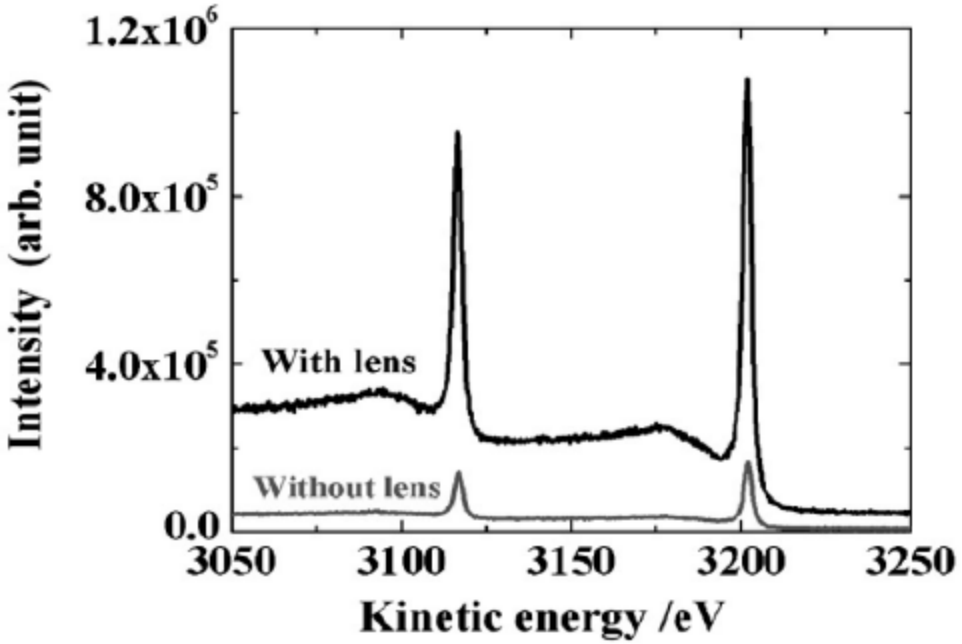

Fig. 4 Au 3d spectra measured with and without the wide acceptance objective lens by Cr K_α excitations of 50 W and 200 µm spot size. These spectra were recorded at 200 eV pass energy and 1.5 mm slit-width, and the electron take-off-angle was 80°.

M. Kobata et al., Analytical Sciences (Japan) 26(2010)227

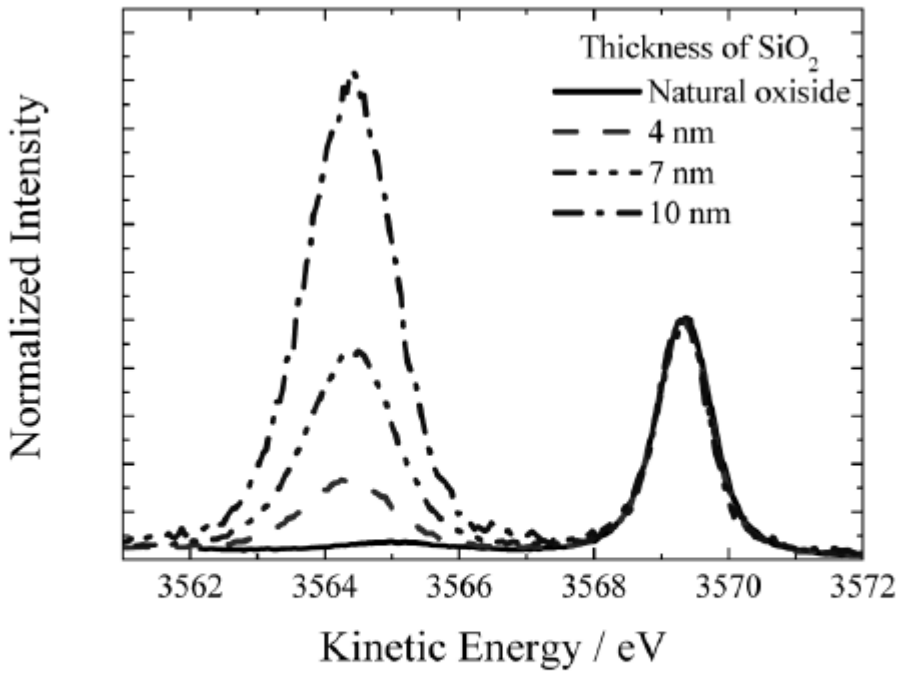

Fig. 7 Si 1s spectra of a Si(001) substrate covered with SiO_2 layers of various thicknesses. These spectra were recorded at 200 eV pass energy and 0.8 mm slit-width, and the electron take-off-angle was 80°.

M. Kobata et al., Analytical Sciences (Japan) 26(2010)227